Principles of Fluorescence Spectroscopy

Third Edition

Principles of Fluorescence Spectroscopy

Third Edition

Joseph R. Lakowicz

University of Maryland School of Medicine
Baltimore, Maryland, USA

Springer

Joseph R. Lakowicz
Center for Fluorescence Spectroscopy
University of Maryland School of Medicine
Baltimore, MD 21201
USA

Library of Congress Control Number: 2006920796

ISBN-10: 0-387-31278-1
ISBN-13: 978-0387-31278-1

Printed on acid-free paper.

Printed in Singapore. (KYO)

9 8 7 6 5 4 3 2 1

springer.com

Dedicated to Mary,
for her continuous support and encouragement,
without whom this book would not have been written

Preface

The first edition of *Principles* was published in 1983, and the second edition 16 years later in 1999. At that time I thought the third edition would not be written until 2010 or later. However, the technology of fluorescence has advanced at an accelerating pace. Single-molecule detection and fluorescence-correlation spectroscopy are becoming almost routine. New classes of probes have appeared, such as the semiconductor nanoparticles, or QDots, and genetically engineered green fluorescent probes. Additionally, it is now becoming possible to control the excited states of fluorophores, rather than relying only on spontaneous emission. These developments are changing the paradigm of fluorescence, from a reliance on organic fluorophores, to the use of genetic engineering, nanotechnology, and near-field optics.

I wish to express my appreciation and special thanks to the individuals who have assisted me in the preparation of the book. These include Ignacy Gryczynski for assistance with the figures, Krystyna Gryczynski for drawing the figures, Joanna Malicka for proofreading the chapters, Kazik Nowaczyk for the cover design and color digitizing of all figures, Tim Oliver for typesetting, and the NIH for their support of my laboratory. And finally, Mary, for her endless hours of typing, correspondence and support.

Joseph R. Lakowicz

Glossary of Acronyms

A	acceptor
AA	anthranilic acid
2-AA	2-acetylanthracene
Ac	acetonitrile
Ac	acetone or acridine
ACF	acriflavine
AcH	acridinium cation
ACTH	adrenocorticotropin hormone
Alexa-Bz	Alexa-labeled benzodiazepine
ADC	analog-to-digital converter
Adx	adrenodoxin
I-AEDANS	5-((((2-iodoacetyl)amino)ethyl)amino)-naphthalene-1-sulfonic acid
AFA	aminofluoranthene
AN	anthracene
2-AN	2-anilinonaphthalene
2,6-ANS	6-(anilino)naphthalene-2-sulfonic acid
AO	acridine orange or acoustooptic
2-AP	2-aminopurine
4-AP	4-aminophthalimide
APC	allophycocyanin
APDs	avalanche photodiodes
9-AS	9-anthroyloxy stearic acid
ASEs	asymptotic standard errors
AT	antithrombin
B	benzene
BABAPH	2-(sulfonatobutyl)-7-(dibutylamino)-2-aza-phenanthrene
BABP	sulfonatobutyl)-4-[4'-(dibutylamino)-phenyl]pyridine
BCECF	7'-bis(2-carboxyethyl)-5(6)-carboxyfluores-cein
BSA	bovine serum albumin
BODIPY	refers to a family of dyes based on 1,3,5,7,8-pentamethyl pyrromethene-BF_2, or 4,4-difluoro-4-bora-3a,4a-diaza-s-indacene; BODIPY is a trademark of Molecular Probes Inc.
β-PE	β-phycoerythrin
BPTI	bovine pancreatic trypsin inhibitor
Bromo-PCs	brominated phosphatidylcholines
Bu	butanol
C102	coumarin 102
C152	coumarin 152
C153	coumarin 153
9-CA	9-cyanoanthracene
CaM	calmodulin
cAMP	cyclic AMP
CFD	constant fraction discriminator
CG	calcium green
CHO	Chinese hamster ovary
CC	closed circular
CCDs	charged-coupled devices
CH	cyclohexane
Chol	cholesterol
CLSM	confocal laser scanning microscopy
CNF	carboxynaphthofluorescein
ConA	concanavalin A
CRABPI	cellular retinoic acid binding protein I
CSR	continuous spectral relaxation
CT	charge transfer
CW	continuous wave
D	donor
Dansyl	5-dimethylaminonaphthalene-1-sulfonic acid
DAPI	4',6-diamidino-2-phenylindole
DAS	decay-associated spectra
DBS	4-dimethylamino-4'-bromostilbene
DC	deoxycytosine
DDQ	distance-dependent quenching
DEA	diethylaniline
DEE	diethyl ether
DHE	dihydroequilenin
DHP	dihexadecyl phosphate
DiI or $DiIC_{12}$	1,1'-didodecyl-3,3,3',3'-tetramethy lindo-carbocyanine
DM	dodecylmaltoside
DMA	dimethylaniline
DMAS	N-dimethylaniline sulfonate
DMF	dimethylformamide
DMPC	dimyristoyl-L-α-phosphatidylcholine
DMP	dimethyldiazaperopyrenium
DMSO	dimethyl sulfoxide
DMQ	2,2'-dimethyl-p-quaterphenyl
10-DN	10-doxylnonadecane

DNS	dansyl or 4-dimethylamino-4'-nitrostilbene
DNS-Cl	dansyl chloride
DOS	trans-4-dimethylamino-4'-(1-oxobutyl) stilbene
DPA	9,10-diphenylanthracene
DPA	dipicolinic acid
DPE	dansyl-labeled phosphatidylethanolamine
DPH	1,6-diphenyl-1,3,5-hexatriene
DPO	2,5-diphenyloxazole
DPPC	dipalmitoyl-L-α-phosphatidylcholine
DPPC	dipalmitoylphosphatidylcholine
DP(M,O)PC(E)	dipalmitoyl(myrisotyl, oleayl)-L-α-phosphatidylcholine (ethanolamine)
DTAC	dodecyltrimethylammonium chloride
EA	ethyl acetate
EA	ethanol
EAN	ethylaniline
EB	ethidium bromide
EC	ethylcellulose
ECFP	enhanced cyan fluorescent protein
EDT	1,2-ethanedithiol
EG	ethylene glycol
ELISA	enzyme-linked immunoadsorbent assays
eosin-PE	eosin-phosphatidylethanolamine
EP	1-ethylpyrene
EPE	eosin-labeled phosphatidylethanolamine
ESIPT	excited-state intramolecular proton transfer
ESR	excited-state reaction
EO	electrooptic
EYFP	enhanced yellow fluorescent protein
F	single-letter code for phenylalanine
Fl	fluorescein
Fl-C	fluorescein-labeled catalytic subunit
FABPs	fatty acid binding proteins
FAD	flavin adenine dinucleotide
FC	fura-2 with calcium
FCS	fluorescence correlation spectroscopy
FD	frequency domain
Fn	fibronectin
Fs	femtosecond
FITC	fluorescein-5-isothiocyanate
FLIM	fluorescence-lifetime imaging microscopy
FMN	flavin mononucleotide
FR	folate receptor
FRET	fluorescence-resonance energy transfer
FWHM	full width of half-maximum intensity
4FW	4-fluorotryptophan
GADPH	glyceraldehyde-3-phosphate dehydrogenase
GFP	green fluorescent protein
GGBP	glucose-galactose binding protein
GM	Goppert-Mayer
GOI	gated optical image intensifier
GP	generalized polarization
GPD	glyceraldehyde-3-phosphate dehydrogenase
GPI	glycosylphosphatidylinositol
GuHCI	guanidine hydrochloride
GUVs	giant unilamellar vesicles
H	n-hexane
HDL	high-density lipoprotein
HeCd	helium–cadmium
HG	harmonic generator
HITCI	hexamethylindotricarbocyanine iodide
HLH	human luteinizing hormone
HO	highest occupied
HpRz	hairpin ribozyme
HPTS	1-hydroxypyrene-3,6,8-trisulfonate
hrIFN-γ	human recombinant interferon γ
HSA	human serum albumin
17β-HSD	17β-hydroxysteroid dehydrogenase
hw	half-width
IAEDANS	5-(((2-iodoacetyl)amino)ethyl)amino)-naphthalene-1-sulfonic acid
IAF	5-iodoacetamidofluorescein
ICT	internal charge transfer
IM	insertion mutant
Indo-1-C_{18}	indo-1 with a C_{18} chain
IRF	instrument response function
IXP	isoxanthopterin
KF	Klenow fragment
KSI	3-ketosteroid isomerase
LADH	liver alcohol dehydrogenase
LCAT	lecithin:cholesterol acyltransferase
LDs	laser diodes
LE	locally excited
LEDs	light-emitting diodes
LU	lowest unoccupied
M	monomer
MAI	N-methylquinolinium iodide
MBP	maltose-binding protein
MCA	multichannel analyzer
MCP	microchannel plate
Me	methanol
MEM	method-of-moments
met RS	methionyl-tRNA synthetase
3-MI	3-methyl indole
MLC	metal–ligand complex, usually of a transition metal, Ru, Rh or Os
MLCK	myosin light chain kinase
MLCT	metal–ligand charge transfer (state)
MLE	maximum likelihood estimates
MPE	multiphoton excitation
MPM	multiphoton microscopy
MQAE	6-methoxy-quinolyl acetoethyl ester
MRI	magnetic resonance imaging

NADH	reduced nicotinamide adenine dinucleotide
NATA	N-acetyl-L-tryptophanamide
NATyrA	N-acetyl-L-tyrosinamide
NB	Nile blue
NBD	N-(7-nitrobenz-2-oxa-1,3-diazol-4-yl)
NBD-DG	1-oleoyl-2-hexanoyl-NBD-glycerol
Nd:YAG	neodymium:YAG
NIR	near infrared
NLLS	nonlinear least squares
NMA	N-methylanthraniloyl amide
NO	nitric oxide
NPN	N-phenyl-1-naphthylamine
NR	neutral red
NRP	neuronal receptor peptide
5-NS	5-doxylstearate
OG	Oregon green
OPO	optical parameter oscillator
ORB	octadecyl rhodamine B
Os	osmium
PBFI	potassium-binding benzofuran isophthalate
PC	phosphatidylcholine
PCSC	photon-counting streak camera
PDA	pyrene dodecanoic acid
PDs	photodiodes
PE	phycoerythrin
PE	phosphatidylethanolamine
1PE	one-photon
2PE	two-photon
3PE	three-photon
PET	photoinduced electron transfer
PeCN	3-cyanoperylene
PG	propylene glycol
PGK	phosphoglycerate kinase
Phe(F)	phenylalanine
PK	protein kinase
PKI	protein kinase inhibitor
PMMA	poly(methylmethacrylate)
PMT	photomultiplier tube
POPC	1-palmitoyl-2-oleoylphosphatidylcholine
POPOP	1,4-bis(5-phenyloxazol-2-yl)benzene
PP	pulse picker
PPD	2,5-diphenyl-1,3,4-oxadizole
PPi	pyrophosphate
PPO	2,5-diphenyloxazole
PRODAN	6-propionyl-2-(dimethylamino)-naphthalene
ps	picosecond
PSDF	phase-sensitive detection of fluorescence
PTP	phosphoryl-transfer protein
Py2	pyridine 2
QDs	quantum dots
QTH	quartz–tungsten halogen
RBC	radiation boundary condition
RBL	rat basophilic leukemia
R-PE	R-phycoerythrin
REES	red-edge excitation shifts
Re I	rhenium
RET	resonance energy transfer
RF	radio frequency
RFP	red fluorescent protein
Rh	rhodamine
RhB	rhodamine B
RhG	rhodamine green
R6G	rhodamine 6G
RNase T_1	ribonuclease T_1
RR	rhodamine red
Ru	ruthenium
SAS	species-associated spectra
SBFI	sodium-binding benzofuran isophthalate
SBP	steroid-binding protein
SBS	substrate-binding strand
SC	subtilisin Carlsberg
SDS	sodium dodecylsulfate
SEDA	dapoxyl sulfonyl ethylenediamine
SMD	single-molecule detection
SNAFLs	seminophthofluoresceins
SNARFs	seminaphthorhodafluors
SP	short-pass
SPQ	6-methoxy-N-[3-sulfopyropyl]quinoline
T	tetramer
TAC	time-to-amplitude converter
TCE	trichloroethanol
t-COPA	16-octadecapentaenoic acid
TCSPC	time-correlated single photon counting
TD	time-domain
TEOS	tetraethylorthosilicate
TFA	trifluoroacetamide
TFE	trifluoroethanol
THF	tetrahydrofuron
TICT	twisted internal charge transfer
TK	thymidine kinase
TL	tear lipocalin
TMA	donor alone
TMR	tetramethylrhodamine
TnC	troponin C
TNS	6-(p-toluidinyl)naphthalene-2-sulfonic acid
TOAH	tetraoctylammonium hydroxide
TOE	tryptophan octyl ester
TPI	triosephosphate isomerase

TRES	time-resolved emission spectra
$TrpNH_2$	tryptophanamide
TRITC	tetramethylrhodamine-5-(and-6)-isothiocyanate
$tRNA^{fMet}$	methionine tRNA
trp(w)	tryptophan
TTS	transit time spread
TU2D	donor–acceptor pair
tyr(y)	tyrosine
U	uridine
7- UmP	7-umbelliferyl phosphate
w	single-letter code for tryptophan
W	water
WT	wild type
WD	window discriminator
Xe	xenon
y	single-letter code for tryptophan
YFP	yellow fluorescent protein

Glossary of Mathematical Terms

A	acceptor or absorption
B_i	brightness of a fluorophore
c	speed of light
C_0	characteristic acceptor concentration in RET
$C(t)$	correlation function for spectral relaxation
D	donor, or diffusion coefficient, or rotational diffusion coefficient
$D_\parallel$ or $D_\perp$	rate of rotation diffusion around or (displacing) the symmetry axis of an ellipsoid of revolution
$D(\tau)$	part of the autocorrelation function for diffusion containing the diffusion-dependent terms
E	efficiency of energy transfer
F	steady-state intensity or fluorescence
$F\chi$	ratio of χ_R^2 values, used to calculate parameter confidence intervals
$F(\lambda)$	emission spectrum
f_i	fractional steady-state intensities in a multi-exponential intensity decay
f_Q	efficiency of collisional quenching
G	correction factor for anisotropy measurements
$G(\tau)$	autocorrelation function of fluorescence fluctuations
hw	half-width in a distance or lifetime distribution
$I(t)$	intensity decay, typically the impulse response function
k_{nr}	non-radiative decay rate
k_s	solvent relaxation rate
k_T	transfer rate in resonance energy transfer
k_{st}	rate of singlet to triplet intersystem crossing
k_{ts}	rate of return to the singlet ground state from the triplet state
m_ω	modulation at a light modulation frequency ω
n	refractive index, when used in consideration of solvent effects
N	number of observed molecules in FCS
$N(t_k)$	number of counts per channel, in time-correlation single-photon counting
$P(r)$	probability function for a distance (r) distribution
pK_a	acid dissociation constant, negative logarithm
q	efficiency for detection of emitted photons, typically for FCS
Q	quantum yield
r	anisotropy (sometimes distance in a distance distribution)
$\bar{r}$	average distance in a distance distribution
$r(0)$	time-zero anisotropy
$r(t)$	anisotropy decay
r_c	distance of closest approach between donors and acceptors in resonance energy transfer, or fluorophores and quenchers
r_{0i} or $r_0 g_i$	fractional amplitudes in a multi-exponential anisotropy decay
r_0	fundamental anisotropy in the absence of rotational diffusion
r_{0i}	anisotropy amplitudes in a multi-exponential anisotropy decay
r_∞	long-time anisotropy in an anisotropy decay
r_ω	modulated anisotropy
R_0	Förster distance in resonance energy transfer
T	temperature
T_P	phase transition temperature for a membrane
α_i	pre-exponential factors in a multi-exponential intensity decay
β	angle between absorption and emission transition moments
γ	inverse of the decay time, $\gamma = 1/\tau$
Γ	radiative decay rate
ε	dielectric constant or extinction coefficient
ε_A or ε	molar extinction coefficient for absorption
θ	rotational correlation time
θ_c	critical angle for total internal reflection
κ^2	orientation factor in resonance energy transfer
λ	wavelength
λ_{em}	emission wavelength
λ_{em}^{max}	maximum emission wavelength
λ_{ex}	excitation wavelength

λ_{ex}^{max}	maximum excitation or absorption wavelength for the lowest $S_0 \rightarrow S_1$ transition
λ_{max}	emission maxima
$\Lambda_?$	ratio of the modulated amplitudes of the polarized components of the emission
η	viscosity
μ_E	excited-state dipole moment
μ_G	ground-state dipole moment
μm	micron
$\bar{\nu}$	specific gravity or wavelength in cm^{-1}
$\bar{\nu}_{cg}$	center of gravity of an emission spectrum in cm^{-1}
σ or σ_A	optical cross-section for absorption
σ_S	optical cross-section for scattering
τ	lifetime or time-delay in FCS
τ_D	diffusion time in FCS
τ_s	solvent or spectral relaxation time

Contents

3. Fluorophores

4. Time-Domain Lifetime Measurements

5. Frequency-Domain Lifetime Measurements

6. Solvent and Environmental Effects

7. Dynamics of Solvent and Spectral Relaxation

8. Quenching of Fluorescence

11. Time-Dependent Anisotropy Decays

12. Advanced Anisotropy Concepts

13. Energy Transfer

14. Time-Resolved Energy Transfer and Conformational Distributions of Biopolymers

15. Energy Transfer to Multiple Acceptors in One, Two, or Three Dimensions

16. Protein Fluorescence

17. Time-Resolved Protein Fluorescence

18. Multiphoton Excitation and Microscopy

19. Fluorescence Sensing

20. Novel Fluorophores

21. DNA Technology

22. Fluorescence-Lifetime Imaging Microscopy

23. Single-Molecule Detection

24. Fluorescence Correlation Spectroscopy

25. Radiative Decay Engineering: Metal-Enhanced Fluorescence

26. Radiative Decay Engineering: Surface Plasmon-Coupled Emission

Appendix I. Corrected Emission Spectra

Appendix II. Fluorescent Lifetime Standards

Appendix III. Additional Reading

1 Introduction to Fluorescence

During the past 20 years there has been a remarkable growth in the use of fluorescence in the biological sciences. Fluorescence spectroscopy and time-resolved fluorescence are considered to be primarily research tools in biochemistry and biophysics. This emphasis has changed, and the use of fluorescence has expanded. Fluorescence is now a dominant methodology used extensively in biotechnology, flow cytometry, medical diagnostics, DNA sequencing, forensics, and genetic analysis, to name a few. Fluorescence detection is highly sensitive, and there is no longer the need for the expense and difficulties of handling radioactive tracers for most biochemical measurements. There has been dramatic growth in the use of fluorescence for cellular and molecular imaging. Fluorescence imaging can reveal the localization and measurements of intracellular molecules, sometimes at the level of single-molecule detection.

Fluorescence technology is used by scientists from many disciplines. This volume describes the principles of fluorescence that underlie its uses in the biological and chemical sciences. Throughout the book we have included examples that illustrate how the principles are used in different applications.

1.1. PHENOMENA OF FLUORESCENCE

Luminescence is the emission of light from any substance, and occurs from electronically excited states. Luminescence is formally divided into two categories—fluorescence and phosphorescence—depending on the nature of the excited state. In excited singlet states, the electron in the excited orbital is paired (by opposite spin) to the second electron in the ground-state orbital. Consequently, return to the ground state is spin allowed and occurs rapidly by emission of a photon. The emission rates of fluorescence are typically 10^8 s^{-1}, so that a typical fluorescence lifetime is near 10 ns (10×10^{-9} s). As will be described in Chapter 4, the lifetime (τ) of a fluorophore is the average time between its excitation and return to the ground state. It is valuable to consider a 1-ns lifetime within the context of the speed of light. Light travels 30 cm, or about one foot, in one nanosecond. Many fluorophores display subnanosecond lifetimes. Because of the short timescale of fluorescence, measurement of the time-resolved emission requires sophisticated optics and electronics. In spite of the added complexity, time-resolved fluorescence is widely used because of the increased information available from the data, as compared with stationary or steady-state measurements. Additionally, advances in technology have made time-resolved measurements easier, even when using microscopes.

Phosphorescence is emission of light from triplet excited states, in which the electron in the excited orbital has the same spin orientation as the ground-state electron. Transitions to the ground state are forbidden and the emission rates are slow (10^3 to 10^0 s^{-1}), so that phosphorescence lifetimes are typically milliseconds to seconds. Even longer lifetimes are possible, as is seen from "glow-in-the-dark" toys. Following exposure to light, the phosphorescence substances glow for several minutes while the excited phosphors slowly return to the ground state. Phosphorescence is usually not seen in fluid solutions at room temperature. This is because there exist many deactivation processes that compete with emission, such as non-radiative decay and quenching processes. It should be noted that the distinction between fluorescence and phosphorescence is not always clear. Transition metal–ligand complexes (MLCs), which contain a metal and one or more organic ligands, display mixed singlet–triplet states. These MLCs display intermediate lifetimes of hundreds of nanoseconds to several microseconds. In this book we will concentrate mainly on the more rapid phenomenon of fluorescence.

Fluorescence typically occurs from aromatic molecules. Some typical fluorescent substances (fluorophores) are shown in Figure 1.1. One widely encountered fluorophore is quinine, which is present in tonic water. If one observes a glass of tonic water that is exposed to sunlight, a faint blue glow is frequently visible at the surface. This glow is most apparent when the glass is observed at a right

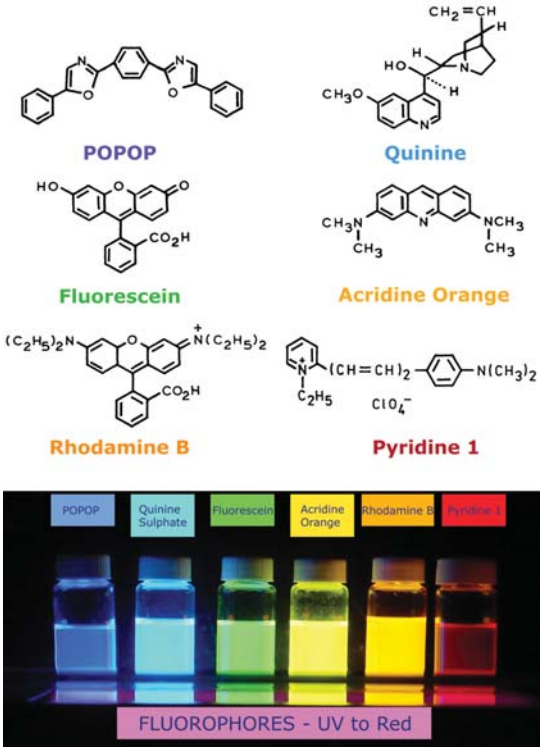

Figure 1.1. Structures of typical fluorescent substances.

Figure 1.2. Sir John Fredrich William Herschel, March 7, 1792 to May 11, 1871. Reproduced courtesy of the Library and Information Centre, Royal Society of Chemistry.

angle relative to the direction of the sunlight, and when the dielectric constant is decreased by adding less polar solvents like alcohols. The quinine in tonic water is excited by the ultraviolet light from the sun. Upon return to the ground state the quinine emits blue light with a wavelength near 450 nm. The first observation of fluorescence from a quinine solution in sunlight was reported by Sir John Frederick William Herschel (Figure 1.2) in 1845.[1] The following is an excerpt from this early report:

> *On a case of superficial colour presented by a homogeneous liquid internally colourless. By Sir John Frederick William Herschel, Philosophical Translation of the Royal Society of London (1845) 135:143–145. Received January 28, 1845 — Read February 13, 1845.*
>
> "The sulphate of quinine is well known to be of extremely sparing solubility in water. It is however easily and copiously soluble in tartaric acid. Equal weights of the sulphate and of crystallised tartaric acid, rubbed up together with addition of a very little water, dissolve entirely and immediately. It is this solution, largely diluted, which exhibits the optical phenomenon in question. Though perfectly transparent and colourless when held between the eye and the light, or a white object, it yet exhibits in certain aspects, and under certain incidences of the light, an extremely vivid and beautiful celestial blue colour, which, from the circumstances of its occurrence, would seem to originate in those strata which the light first penetrates in entering the liquid, and which, if not strictly superficial, at least exert their peculiar power of analysing the incident rays and dispersing those which compose the tint in question, only through a very small depth within the medium.
>
> To see the colour in question to advantage, all that is requisite is to dissolve the two ingredients above mentioned in equal proportions, in about a hundred times their joint weight of water, and having filtered the solution, pour it into a tall narrow cylindrical glass vessel or test tube, which is to be set upright on a dark coloured substance before an open window exposed to strong daylight or sunshine, but with no cross lights, or any strong reflected light from behind. If we look down perpendicularly into the vessel so that the visual ray shall graze the internal surface of the glass through a great part of its depth, the whole of that surface of the liquid on which the light first strikes will appear of a lively blue, ...
>
> If the liquid be poured out into another vessel, the descending stream gleams internally from all

> its undulating inequalities, with the same lively yet delicate blue colour, ... thus clearly demonstrating that contact with a denser medium has no share in producing this singular phenomenon.
>
> The thinnest film of the liquid seems quite as effective in producing this superficial colour as a considerable thickness. For instance, if in pouring it from one glass into another, ... the end of the funnel be made to touch the internal surface of the vessel well moistened, so as to spread the descending stream over an extensive surface, the intensity of the colour is such that it is almost impossible to avoid supposing that we have a highly coloured liquid under our view."

It is evident from this early description that Sir Herschel recognized the presence of an unusual phenomenon that could not be explained by the scientific knowledge of the time. To this day the fluorescence of quinine remains one of the most used and most beautiful examples of fluorescence. Herschel was from a distinguished family of scientists who lived in England but had their roots in Germany.[2] For most of his life Sir Herschel did research in astronomy, publishing only a few papers on fluorescence.

It is interesting to notice that the first known fluorophore, quinine, was responsible for stimulating the development of the first spectrofluorometers that appeared in the 1950s. During World War II, the Department of War was interested in monitoring antimalaria drugs, including quinine. This early drug assay resulted in a subsequent program at the National Institutes of Health to develop the first practical spectrofluorometer.[3]

Many other fluorophores are encountered in daily life. The green or red-orange glow sometimes seen in antifreeze is due to trace quantities of fluorescein or rhodamine, respectively (Figure 1.1). Polynuclear aromatic hydrocarbons, such as anthracene and perylene, are also fluorescent, and the emission from such species is used for environmental monitoring of oil pollution. Some substituted organic compounds are also fluorescent. For example 1,4-bis(5-phenyloxazol-2-yl)benzene (POPOP) is used in scintillation counting and acridine orange is often used as a DNA stain. Pyridine 1 and rhodamine are frequently used in dye lasers.

Numerous additional examples of probes could be presented. Instead of listing them here, examples will appear throughout the book, with a description of the spectral properties of the individual fluorophores. An overview of fluorophores used for research and fluorescence sensing is presented in Chapter 3. In contrast to aromatic organic molecules, atoms are generally nonfluorescent in condensed phases. One notable exception is the group of elements commonly known as the lanthanides.[4] The fluorescence from europium and terbium ions results from electronic transitions between *f* orbitals. These orbitals are shielded from the solvent by higher filled orbitals. The lanthanides display long decay times because of this shielding and low emission rates because of their small extinction coefficients.

Fluorescence spectral data are generally presented as emission spectra. A fluorescence emission spectrum is a plot of the fluorescence intensity versus wavelength (nanometers) or wavenumber (cm^{-1}). Two typical fluorescence emission spectra are shown in Figure 1.3. Emission spectra vary widely and are dependent upon the chemical structure of the fluorophore and the solvent in which it is dissolved. The spectra of some compounds, such as perylene, show significant structure due to the individual vibrational energy levels of the ground and excited states. Other compounds, such as quinine, show spectra devoid of vibrational structure.

An important feature of fluorescence is high sensitivity detection. The sensitivity of fluorescence was used in 1877 to demonstrate that the rivers Danube and Rhine were connected by underground streams.[5] This connection was demonstrated by placing fluorescein (Figure 1.1) into the Danube. Some sixty hours later its characteristic green fluorescence appeared in a small river that led to the Rhine. Today fluorescein is still used as an emergency marker for locating individuals at sea, as has been seen on the landing of space capsules in the Atlantic Ocean. Readers interested in the history of fluorescence are referred to the excellent summary by Berlman.[5]

1.2. JABLONSKI DIAGRAM

The processes that occur between the absorption and emission of light are usually illustrated by the Jablonski[6] diagram. Jablonski diagrams are often used as the starting point for discussing light absorption and emission. Jablonski diagrams are used in a variety of forms, to illustrate various molecular processes that can occur in excited states. These diagrams are named after Professor Alexander Jablonski (Figure 1.4), who is regarded as the father of fluorescence spectroscopy because of his many accomplishments, including descriptions of concentration depolarization and defining the term "anisotropy" to describe the polarized emission from solutions.[7,8]

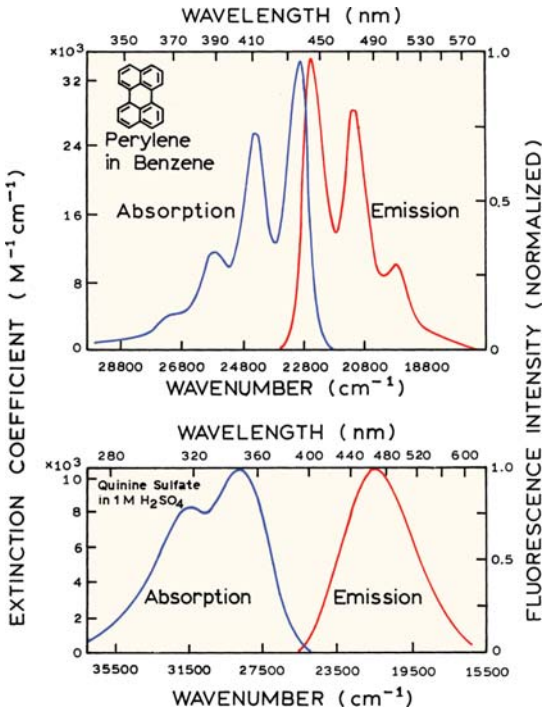

Figure 1.3. Absorption and fluorescence emission spectra of perylene and quinine. Emission spectra cannot be correctly presented on both the wavelength and wavenumber scales. The wavenumber presentation is correct in this instance. Wavelengths are shown for convenience. See Chapter 3. Revised from [5].

Brief History of Alexander Jablonski

Professor Jablonski was born February 26, 1898 in Voskresenovka, Ukraine. In 1916 he began his study of atomic physics at the University of Kharkov, which was interrupted by military service first in the Russian Army and later in the newly organized Polish Army during World War I. At the end of 1918, when an independent Poland was re-created after more than 120 years of occupation by neighboring powers, Jablonski left Kharkov and arrived in Warsaw, where he entered the University of Warsaw to continue his study of physics. His study in Warsaw was again interrupted in 1920 by military service during the Polish-Bolshevik war.

An enthusiastic musician, Jablonski played first violin at the Warsaw Opera from 1921 to 1926 while studying at the university under Stefan Pienkowski. He received his doctorate in 1930 for work "On the influence of the change of wavelengths of excitation light on the fluorescence spectra." Although Jablonski left the opera in 1926 and devoted himself entirely to scientific work, music remained his great passion until the last days of his life.

Figure 1.4. Professor Alexander Jablonski (1898–1980), circa 1935. Courtesy of his daughter, Professor Danuta Frackowiak.

Throughout the 1920s and 30s the Department of Experimental Physics at Warsaw University was an active center for studies on luminescence under S. Pienkowski. During most of this period Jablonski worked both theoretically and experimentally on the fundamental problems of photoluminescence of liquid solutions as well as on the pressure effects on atomic spectral lines in gases. A problem that intrigued Jablonski for many years was the polarization of photoluminescence of solutions. To explain the experimental facts he distinguished the transition moments in absorption and in emission and analyzed various factors responsible for the depolarization of luminescence.

Jablonski's work was interrupted once again by a world war. From 1939 to 1945 Jablonski served in the Polish Army, and spent time as a prisoner of first the German Army and then the Soviet Army. In 1946 he returned to Poland to chair a new Department of Physics in the new Nicholas Copernicus University in Torun. This beginning occurred in the very difficult postwar years in a country totally destroyed by World War II. Despite all these difficulties, Jablonski with great energy organized the Department of Physics at the university, which became a scientific center for studies in atomic and molecular physics.

His work continued beyond his retirement in 1968. Professor Jablonski created a spectroscopic school of thought that persists today through his numerous students, who now occupy positions at universities in Poland and elsewhere. Professor Jablonski died on September 9, 1980. More complete accounts of his accomplishments are given in [7] and [8].

A typical Jablonski diagram is shown in Figure 1.5. The singlet ground, first, and second electronic states are depicted by S_0, S_1, and S_2, respectively. At each of these electronic energy levels the fluorophores can exist in a number of vibrational energy levels, depicted by 0, 1, 2, etc. In this Jablonski diagram we excluded a number of interactions that will be discussed in subsequent chapters, such as quenching, energy transfer, and solvent interactions. The transitions between states are depicted as vertical lines to illustrate the instantaneous nature of light absorption. Transitions occur in about 10^{-15} s, a time too short for significant displacement of nuclei. This is the Franck-Condon principle.

The energy spacing between the various vibrational energy levels is illustrated by the emission spectrum of perylene (Figure 1.3). The individual emission maxima (and hence vibrational energy levels) are about 1500 cm^{-1} apart. At room temperature thermal energy is not adequate to significantly populate the excited vibrational states. Absorption and emission occur mostly from molecules with the lowest vibrational energy. The larger energy difference between the S_0 and S_1 excited states is too large for thermal population of S_1. For this reason we use light and not heat to induce fluorescence.

Following light absorption, several processes usually occur. A fluorophore is usually excited to some higher vibrational level of either S_1 or S_2. With a few rare exceptions, molecules in condensed phases rapidly relax to the lowest vibrational level of S_1. This process is called internal conversion and generally occurs within 10^{-12} s or less. Since fluorescence lifetimes are typically near 10^{-8} s, internal conversion is generally complete prior to emission. Hence, fluorescence emission generally results from a thermally equilibrated excited state, that is, the lowest energy vibrational state of S_1.

Return to the ground state typically occurs to a higher excited vibrational ground state level, which then quickly (10^{-12} s) reaches thermal equilibrium (Figure 1.5). Return to an excited vibrational state at the level of the S_0 state is the reason for the vibrational structure in the emission spectrum of perylene. An interesting consequence of emission to higher vibrational ground states is that the emission spectrum is typically a mirror image of the absorption spectrum of the $S_0 \rightarrow S_1$ transition. This similarity occurs because electronic excitation does not greatly alter the nuclear geometry. Hence the spacing of the vibrational energy levels of the excited states is similar to that of the ground state. As a result, the vibrational structures seen in the absorption and the emission spectra are similar.

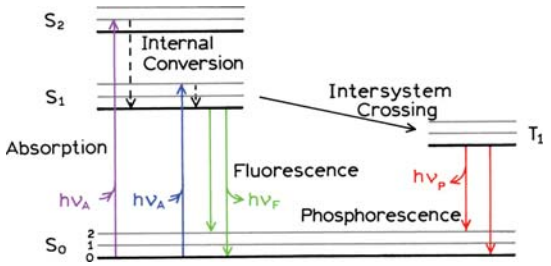

Figure 1.5. One form of a Jablonski diagram.

Molecules in the S_1 state can also undergo a spin conversion to the first triplet state T_1. Emission from T_1 is termed phosphorescence, and is generally shifted to longer wavelengths (lower energy) relative to the fluorescence. Conversion of S_1 to T_1 is called intersystem crossing. Transition from T_1 to the singlet ground state is forbidden, and as a result the rate constants for triplet emission are several orders of magnitude smaller than those for fluorescence. Molecules containing heavy atoms such as bromine and iodine are frequently phosphorescent. The heavy atoms facilitate intersystem crossing and thus enhance phosphorescence quantum yields.

1.3. CHARACTERISTICS OF FLUORESCENCE EMISSION

The phenomenon of fluorescence displays a number of general characteristics. Exceptions are known, but these are infrequent. Generally, if any of the characteristics described in the following sections are not displayed by a given fluorophore, one may infer some special behavior for this compound.

1.3.1. The Stokes Shift

Examination of the Jablonski diagram (Figure 1.5) reveals that the energy of the emission is typically less than that of absorption. Fluorescence typically occurs at lower energies or longer wavelengths. This phenomenon was first observed by Sir. G. G. Stokes in 1852 at the University of Cambridge.[9] These early experiments used relatively simple

instrumentation (Figure 1.6). The source of ultraviolet excitation was provided by sunlight and a blue glass filter, which was part of a stained glass window. This filter selectively transmitted light below 400 nm, which was absorbed by quinine (Figure 1.6). The incident light was prevented from reaching the detector (eye) by a yellow glass (of wine) filter. Quinine fluorescence occurs near 450 nm and is therefore easily visible.

It is interesting to read Sir George's description of the observation. The following is from his report published in 1852:[9]

> *On the Change of Refrangibility of Light. By G. G. Stokes, M.A., F.R.S., Fellow of Pembroke College, and Lucasian Professor of Mathematics in the University of Cambridge. Phil. Trans. Royal Society of London (1852) pp. 463-562. Received May 11, — Read May 27, 1852.*
>
> "The following researches originated in a consideration of the very remarkable phenomenon discovered by Sir John Herschel in a solution of sulphate of quinine, and described by him in two papers printed in the Philosophical Transactions for 1845, entitled "On a Case of Superficial Colour presented by a Homogeneous Liquid internally colourless," and "On the Epipolic Dispersion of Light." The solution of quinine, though it appears to be perfectly transparent and colourless, like water, when viewed by transmitted light, exhibits nevertheless in certain aspects, and under certain incidences of the light, a beautiful celestial blue colour. It appears from the experiments of Sir John Herschel that the blue colour comes only from a stratum of fluid of small but finite thickness adjacent to the surface by which the light enters. After passing through this stratum, the incident light, though not sensibly enfeebled nor coloured, has lost the power of producing the same effect, and therefore may be considered as in some way or other qualitatively different from the original light."

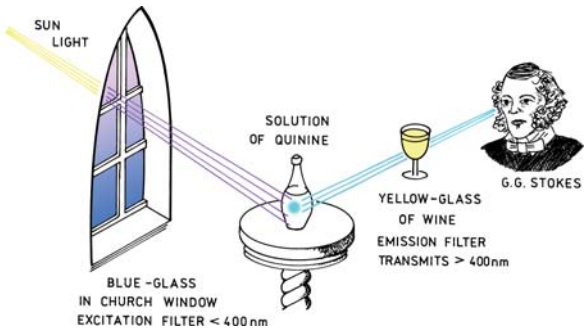

Figure 1.6. Experimental schematic for detection of the Stokes shift.

Careful reading of this paragraph reveals several important characteristics of fluorescent solutions. The quinine solution is colorless because it absorbs in the ultraviolet, which we cannot see. The blue color comes only from a region near the surface. This is because the quinine solution was relatively concentrated and absorbed all of the UV in the first several millimeters. Hence Stokes observed the inner filter effect. After passing through the solution the light was "enfeebled" and no longer capable of causing the blue glow. This occurred because the UV was removed and the "enfeebled" light could no longer excite quinine. However, had Sir George used a second solution of fluorescein, rather than quinine, it would have still been excited because of the longer absorption wavelength of fluorescein.

Energy losses between excitation and emission are observed universally for fluorescent molecules in solution. One common cause of the Stokes shift is the rapid decay to the lowest vibrational level of S_1. Furthermore, fluorophores generally decay to higher vibrational levels of S_0 (Figure 1.5), resulting in further loss of excitation energy by thermalization of the excess vibrational energy. In addition to these effects, fluorophores can display further Stokes shifts due to solvent effects, excited-state reactions, complex formation, and/or energy transfer.

Brief History of Sir. G. G. Stokes:

Professor Stokes was born in Ireland, August 3, 1819 (Figure 1.7). He entered Pembroke College, Cambridge, in 1837, and was elected as a fellow of Pembroke immediately upon his graduation in 1841. In 1849 Stokes became Lucasian Professor at Cambridge, a chair once held by Newton. Because of poor endowment for the chair, he also worked in the Government School of Mines.

Stokes was involved with a wide range of scientific problems, including hydrodynamics, elasticity of solids, and diffraction of light. The wave theory of light was already known when he entered Cambridge. In his classic paper on quinine, he understood that light of a higher "refrangibility" or frequency was responsible for the blue glow of lower refrangibility or frequency. Thus invisible ultraviolet rays were absorbed to produce the blue light at the surface. Stokes later suggested using optical properties such as absorption, colored reflection, and fluorescence, to identify organic substances.

Later in life Stokes was universally honored with degrees and medals. He was knighted in 1889 and became Master of Pembroke College in 1902. After the 1850s, Stokes became involved in administrative matters, and his scientific productivity decreased. Some things never change. Professor Stokes died February 1, 1903.

Figure 1.7. Sir George Gabriel Stokes, 1819–1903, Lucasian Professor at Cambridge. Reproduced courtesy of the Library and Information Centre, Royal Society of Chemistry.

1.3.2. Emission Spectra Are Typically Independent of the Excitation Wavelength

Another general property of fluorescence is that the same fluorescence emission spectrum is generally observed irrespective of the excitation wavelength. This is known as Kasha's rule,[10] although Vavilov reported in 1926 that quantum yields were generally independent of excitation wavelength.[5] Upon excitation into higher electronic and vibrational levels, the excess energy is quickly dissipated, leaving the fluorophore in the lowest vibrational level of S_1. This relaxation occurs in about 10^{-12} s, and is presumably a result of a strong overlap among numerous states of nearly equal energy. Because of this rapid relaxation, emission spectra are usually independent of the excitation wavelength. Exceptions exist, such as fluorophores that exist in two ionization states, each of which displays distinct absorption and emission spectra. Also, some molecules are known to emit from the S_2 level, but such emission is rare and generally not observed in biological molecules.

It is interesting to ask why perylene follows the mirror-image rule, but quinine emission lacks the two peaks seen in its excitation spectrum at 315 and 340 nm (Figure 1.3). In the case of quinine, the shorter wavelength absorption peak is due to excitation to the second excited state (S_2), which relaxes rapidly to S_1. Emission occurs predominantly from the lowest singlet state (S_1), so emission from S_2 is not observed. The emission spectrum of quinine is the mirror image of the $S_0 \rightarrow S_1$ absorption of quinine, not of its total absorption spectrum. This is true for most fluorophores: the emission is the mirror image of $S_0 \rightarrow S_1$ absorption, not of the total absorption spectrum.

The generally symmetric nature of these spectra is a result of the same transitions being involved in both absorption and emission, and the similar vibrational energy levels of S_0 and S_1. In most fluorophores these energy levels are not significantly altered by the different electronic distributions of S_0 and S_1. Suppose the absorption spectrum of a fluorophore shows distinct peaks due to the vibrational energy levels. Such peaks are seen for anthracene in Figure 1.8. These peaks are due to transitions from the lowest vibrational level of the S_0 state to higher vibrational levels of the S_1 state. Upon return to the S_0 state the fluorophore can return to any of the ground state vibrational levels. These vibrational energy levels have similar spacing to those in the S_1 state. The emission spectrum shows the same vibrational energy spacing as the absorption spectrum. According to the Franck-Condon principle, all electronic transitions are vertical, that is, they occur without change in the position of the nuclei. As a result, if a particular transition probability (Franck-Condon factor) between the 0th and 1st vibrational levels is largest in absorption, the reciprocal transition is also most probable in emission (Figure 1.8).

A rigorous test of the mirror-image rule requires that the absorption and emission spectra be presented in appropriate units.[12] The closest symmetry should exist between the modified spectra $\varepsilon(\bar{\nu})/\bar{\nu}$ and $F(\bar{\nu})/\bar{\nu}^3$, where $\varepsilon(\bar{\nu})$ is the extinction coefficient at wavenumber ($\bar{\nu}$), and $F(\bar{\nu})$ is the relative photon flux over a wavenumber increment $\Delta\bar{\nu}$. Agreement between these spectra is generally found for polynuclear aromatic hydrocarbons.

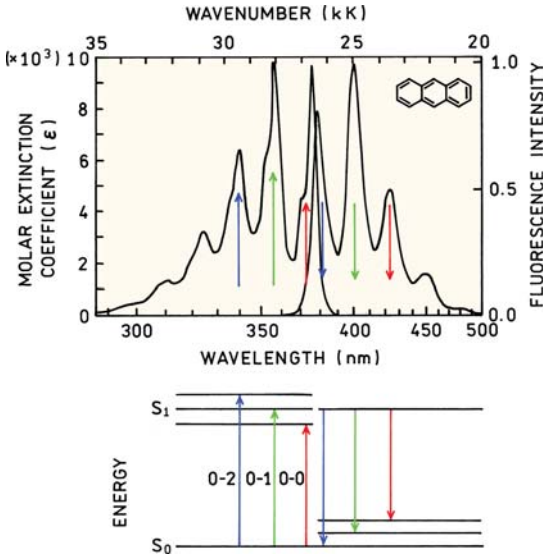

Figure 1.8. Mirror-image rule and Franck-Condon factors. The absorption and emission spectra are for anthracene. The numbers 0, 1, and 2 refer to vibrational energy levels. From [11].

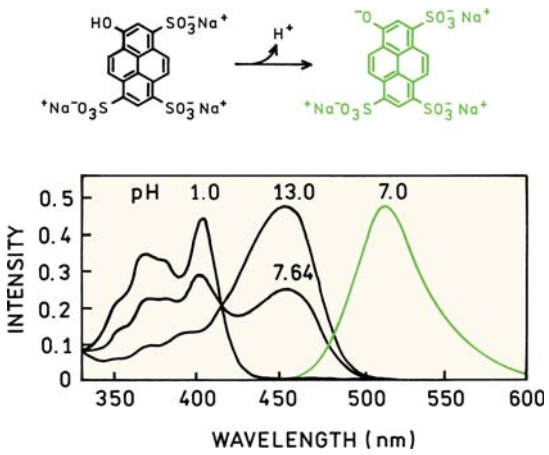

Figure 1.9. Absorption (pH 1, 7.64, and 13) and emission spectra (pH 7) of 1-hydroxypyrene-3,6,8-trisulfonate in water. From [11].

1.3.3. Exceptions to the Mirror-Image Rule

Although often true, many exceptions to the mirror-image rule occur. This is illustrated for the pH-sensitive fluorophore 1-hydroxypyrene-3,6,8-trisulfonate (HPTS) in Figure 1.9. At low pH the hydroxyl group is protonated. The absorption spectrum at low pH shows vibrational structure typical of an aromatic hydrocarbon. The emission spectrum shows a large Stokes shift and none of the vibrational structure seen in the absorption spectrum. The difference between the absorption emission spectra is due to ionization of the hydroxyl group. The dissociation constant (pK_a) of the hydroxyl group decreases in the excited state, and this group becomes ionized. The emission occurs from a different molecular species, and this ionized species displays a broad spectrum. This form of HPTS with an ionized hydroxyl group can be formed at pH 13. The emission spectrum is a mirror image of the absorption of the high pH form of HPTS.

Changes in pK_a in the excited state also occur for biochemical fluorophores. For example, phenol and tyrosine each show two emissions, the long-wavelength emission being favored by a high concentration of proton acceptors. The pK_a of the phenolic hydroxyl group decreases from 11 in the ground state to 4 in the excited state. Following excitation, the phenolic proton is lost to proton acceptors in the solution. Depending upon the concentration of these acceptors, either the phenol or the phenolate emission may dominate the emission spectrum.

Excited-state reactions other than proton dissociation can also result in deviations from the mirror symmetry rule. One example is shown in Figure 1.10, which shows the emission spectrum of anthracene in the presence of diethylaniline.[13] The structured emission at shorter wavelengths is a mirror image of the absorption spectrum of anthracene. The unstructured emission at longer wavelengths is due to formation of a charge-transfer complex between the excited state of anthracene and diethylaniline. The unstructured emission is from this complex. Many polynuclear aromatic hydrocarbons, such as pyrene and perylene, also form charge-transfer complexes with amines. These excited-state complexes are referred to as exciplexes.

Some fluorophores can also form complexes with themselves. The best known example is pyrene. At low concentrations pyrene displays a highly structured emission (Figure 1.11). At higher concentrations the previously invisible UV emission of pyrene becomes visible at 470 nm. This long-wavelength emission is due to excimer formation. The term "excimer" is an abbreviation for an excited-state dimer.

1.4. FLUORESCENCE LIFETIMES AND QUANTUM YIELDS

The fluorescence lifetime and quantum yield are perhaps the most important characteristics of a fluorophore. Quantum yield is the number of emitted photons relative to the number of absorbed photons. Substances with the largest quantum yields, approaching unity, such as rhodamines, display the brightest emissions. The lifetime is also important, as it determines the time available for the fluorophore

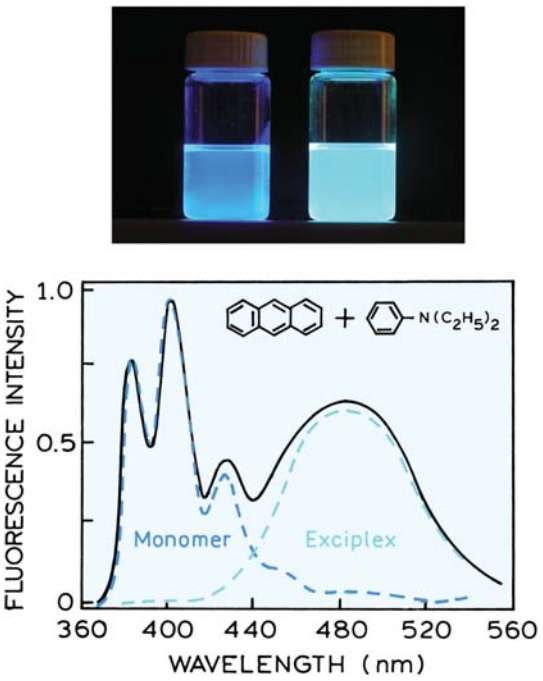

Figure 1.10. Emission spectrum of anthracene in toluene containing 0.2 M diethylaniline. The dashed lines show the emission spectra of anthracene or its exciplex with diethylaniline. Figure revised from [13], photo from [14].

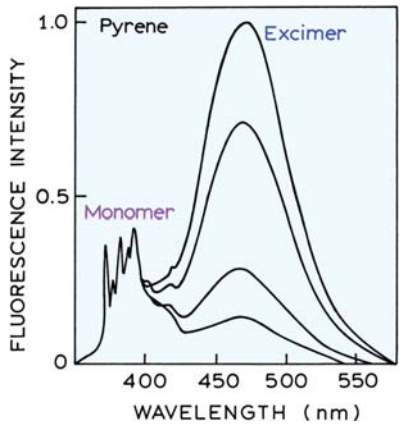

Figure 1.11. Emission spectra of pyrene and its excimer. The relative intensity of the excimer peak (470 nm) decreases as the total concentration of pyrene is decreased from 6 x 10^{-3} M (top) to 0.9 x 10^{-4} M (bottom). Reproduced with permission from John Wiley and Sons Inc. From [12].

to interact with or diffuse in its environment, and hence the information available from its emission.

The meanings of quantum yield and lifetime are best represented by a simplified Jablonski diagram (Figure 1.12). In this diagram we do not explicitly illustrate the individual relaxation processes leading to the relaxed S_1 state. Instead, we focus on those processes responsible for return to the ground state. In particular, we are interested in the emissive rate of the fluorophore (Γ) and its rate of non-radiative decay to S_0 (k_{nr}).

The fluorescence quantum yield is the ratio of the number of photons emitted to the number absorbed. The rate constants Γ and k_{nr} both depopulate the excited state. The fraction of fluorophores that decay through emission, and hence the quantum yield, is given by

$$Q = \frac{\Gamma}{\Gamma + k_{nr}} \tag{1.1}$$

The quantum yield can be close to unity if the radiationless decay rate is much smaller than the rate of radiative decay, that is $k_{nr} < \Gamma$. We note that the energy yield of fluorescence is always less than unity because of Stokes losses. For convenience we have grouped all possible non-radiative decay processes with the single rate constant k_{nr}.

The lifetime of the excited state is defined by the average time the molecule spends in the excited state prior to return to the ground state. Generally, fluorescence lifetimes are near 10 ns. For the fluorophore illustrated in Figure 1.12 the lifetime is

$$\tau = \frac{1}{\Gamma + k_{nr}} \tag{1.2}$$

Fluorescence emission is a random process, and few molecules emit their photons at precisely $t = \tau$. The lifetime is an average value of the time spent in the excited state. For a single exponential decay (eq. 1.13) 63% of the molecules have decayed prior to $t = \tau$ and 37% decay at $t > \tau$.

An example of two similar molecules with different lifetimes and quantum yields is shown in Figure 1.13. The differences in lifetime and quantum yield for eosin and erythrosin B are due to differences in non-radiative decay rates. Eosin and erythrosin B have essentially the same extinction coefficient and the same radiative decay rate (see eq. 1.4). Heavy atoms such as iodine typically result in shorter lifetimes and lower quantum yields.

The lifetime of the fluorophore in the absence of non-radiative processes is called the intrinsic or natural lifetime, and is given by

$$\tau_n = \frac{1}{\Gamma} \tag{1.3}$$

In principle, the natural lifetime τ_n can be calculated from the absorption spectra, extinction coefficient, and

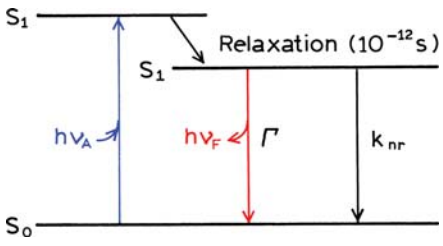

Figure 1.12. A simplified Jablonski diagram to illustrate the meaning of quantum yields and lifetimes.

emission spectra of the fluorophore. The radiative decay rate Γ can be calculated using[15,16]

$$\Gamma \simeq 2.88 \times 10^9 \, n^2 \frac{\int F(\bar{\nu})\, d\bar{\nu}}{\int F(\bar{\nu}) d\bar{\nu}/\bar{\nu}^3} \int \frac{\varepsilon(\bar{\nu})}{\bar{\nu}}\, d\bar{\nu}$$

$$= 2.88 \times 10^9 n^2 \langle \bar{\nu}^{-3} \rangle^{-1} \int \frac{\varepsilon(\bar{\nu})\, d\bar{\nu}}{\bar{\nu}} \qquad (1.4)$$

where $F(\bar{\nu})$ is the emission spectrum plotted on the wavenumber (cm^{-1}) scale, $\varepsilon(\bar{\nu})$ is the absorption spectrum, and n is the refractive index of the medium. The integrals are calculated over the $S_0 \leftrightarrow S_1$ absorption and emission spectra. In many cases this expression works rather well, particularly for solutions of polynuclear aromatic hydrocarbons. For instance, the calculated value[15] of Γ for perylene is 1.8 x 10^8 s^{-1}, which yields a natural lifetime of 5.5 ns. This value is close to that observed for perylene, which displays a quantum yield near unity. However, there are numerous reasons why eq. 1.4 can fail. This expression assumes no interaction with the solvent, does not consider changes in the refractive index (n) between the absorption and emission wavelength, and assumes no change in excited-state geometry. A more complete form of eq. 1.4 (not shown) includes a factor $G = g_l/g_u$ on the right-hand side, where g_l and g_u are the degeneracies of the lower and upper states, respectively. For fluorescence transitions $G = 1$, for phosphorescence transitions $G = 1/3$.

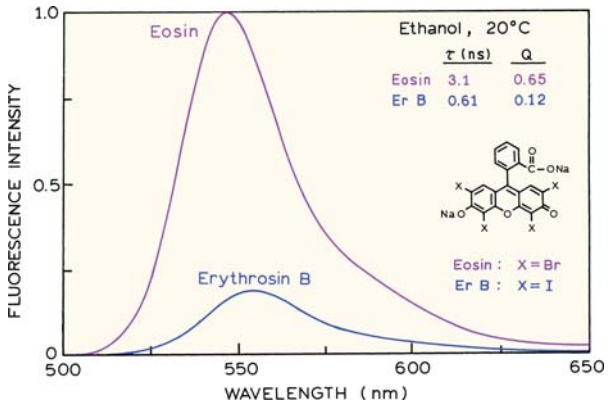

Figure 1.13. Emission spectra of eosin and erythrosin B (ErB).

The natural lifetime can be calculated from the measured lifetime (τ) and quantum yield

$$\tau_n = \tau / Q \qquad (1.5)$$

which can be derived from eqs. 1.2 and 1.3. Many biochemical fluorophores do not behave as predictably as unsubstituted aromatic compounds. Hence, there is often poor agreement between the value of τ_n calculated from eq. 1.5 and that calculated from its absorption and emission spectra (eq. 1.4). These discrepancies occur for a variety of unknown and known reasons, such as a fraction of the fluorophores located next to quenching groups, which sometimes occurs for tryptophan residues in proteins.

The quantum yield and lifetime can be modified by factors that affect either of the rate constants (Γ or k_{nr}). For example, a molecule may be nonfluorescent as a result of a large rate of internal conversion or a slow rate of emission. Scintillators are generally chosen for their high quantum yields. These high yields are a result of large Γ values. Hence, the lifetimes are generally short: near 1 ns. The fluorescence emission of aromatic substances containing $-NO_2$ groups are generally weak, primarily as a result of large k_{nr} values. The quantum yields of phosphorescence are extremely small in fluid solutions at room temperature. The triplet-to-singlet transition is forbidden by symmetry, and the rates of spontaneous emission are about 10^3 s^{-1} or smaller. Since k_{nr} values are near 10^9 s^{-1}, the quantum yields of phosphorescence are small at room temperature. From eq. 1.1 one can predict phosphorescence quantum yields of 10^{-6}.

Comparison of the natural lifetime, measured lifetime, and quantum yield can be informative. For example, in the case of the widely used membrane probe 1,6-diphenyl-1,3,5-hexatriene (DPH) the measured lifetime near 10 ns is much longer than that calculated from eq. 1.4, which is near 1.5 ns.[17] In this case the calculation based on the absorption spectrum of DPH is incorrect because the absorption transition is to a state of different electronic symmetry than the emissive state. Such quantum-mechanical effects are rarely seen in more complex fluorophores with heterocyclic atoms.

1.4.1. Fluorescence Quenching

The intensity of fluorescence can be decreased by a wide variety of processes. Such decreases in intensity are called quenching. Quenching can occur by different mechanisms. Collisional quenching occurs when the excited-state fluorophore is deactivated upon contact with some other molecule in solution, which is called the quencher. Collisional quenching is illustrated on the modified Jablonski diagram in Figure 1.14. In this case the fluorophore is returned to the ground state during a diffusive encounter with the quencher. The molecules are not chemically altered in the process. For collisional quenching the decrease in intensity is described by the well-known Stern-Volmer equation:

$$\frac{F_0}{F} = 1 + K[Q] = 1 + k_q\tau_0[Q] \qquad (1.6)$$

In this expression K is the Stern-Volmer quenching constant, k_q is the bimolecular quenching constant, τ_0 is the unquenched lifetime, and $[Q]$ is the quencher concentration. The Stern-Volmer quenching constant K indicates the sensitivity of the fluorophore to a quencher. A fluorophore buried in a macromolecule is usually inaccessible to water-soluble quenchers, so that the value of K is low. Larger values of K are found if the fluorophore is free in solution or on the surface of a biomolecule.

A wide variety of molecules can act as collisional quenchers. Examples include oxygen, halogens, amines, and electron-deficient molecules like acrylamide. The mechanism of quenching varies with the fluorophore–quencher pair. For instance, quenching of indole by acrylamide is probably due to electron transfer from indole to acrylamide, which does not occur in the ground state. Quenching by halogen and heavy atoms occurs due to spin–orbit coupling and intersystem crossing to the triplet state (Figure 1.5).

Aside from collisional quenching, fluorescence quenching can occur by a variety of other processes. Fluorophores can form nonfluorescent complexes with quenchers. This process is referred to as static quenching since it occurs in the ground state and does not rely on diffusion or molecular collisions. Quenching can also occur by a variety of trivial, i.e., non-molecular mechanisms, such as attenuation of the incident light by the fluorophore itself or other absorbing species.

1.4.2. Timescale of Molecular Processes in Solution

The phenomenon of quenching provides a valuable context for understanding the role of the excited-state lifetime in allowing fluorescence measurements to detect dynamic processes in solution or in macromolecules. The basic idea is that absorption is an instantaneous event. According to the Franck-Condon principle, absorption occurs so fast that there is no time for molecular motion during the absorption process. Absorption occurs in the time it takes a photon to travel the length of a photon: in less than 10^{-15} s. As a result, absorption spectroscopy can only yield information on the average ground state of the molecules that absorb light. Only solvent molecules that are immediately adjacent to the absorbing species will affect its absorption spectrum. Absorption spectra are not sensitive to molecular dynamics and can only provide information on the average solvent shell adjacent to the chromophore.

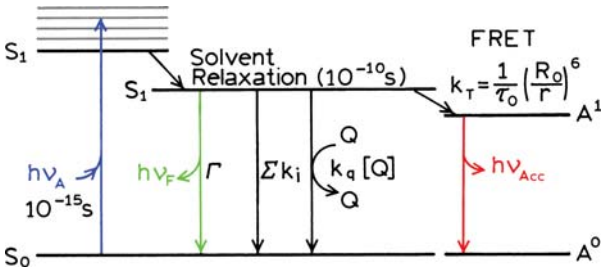

Figure 1.14. Jablonski diagram with collisional quenching and fluorescence resonance energy transfer (FRET). The term Σk_i is used to represent non-radiative paths to the ground state aside from quenching and FRET.

In contrast to absorption, emission occurs over a longer period of time. The length of time fluorescent molecules remain in the excited state provides an opportunity for interactions with other molecules in solution. Collisional quenching of fluorescence by molecular oxygen is an excellent example of the expansion of time and distance provided by the fluorescence lifetime. If a fluorophore in the excited state collides with an oxygen molecule, then the fluorophore returns to the ground state without emission of a photon. The diffusion coefficient (D) of oxygen in water at 25°C is 2.5 x 10^{-5} cm^2/s. Suppose a fluorophore has a lifetime of 10 ns. Although 10 ns may appear to be a brief time span, it is in fact quite long relative to the motions of small molecules in fluid solution. The average distance $(\Delta x^2)^{1/2}$ an oxygen molecule can diffuse in 10^{-8} s or 10 ns is given by the Einstein equation:

$$\Delta x^2 = 2D\tau \qquad (1.7)$$

The distance is about 70 Å, which is comparable to the thickness of a biological membrane or the diameter of a protein. Some fluorophores have lifetimes as long as 400

ns, and hence diffusion of oxygen molecules may be observed over distances of 450 Å. Absorption measurements are only sensitive to the immediate environment around the fluorophore, and then only sensitive to the instantaneously averaged environment.

Other examples of dynamic processes in solution involve fluorophore–solvent interactions and rotational diffusion. As was observed by Stokes, most fluorophores display emission at lower energies than their absorption. Most fluorophores have larger dipole moments in the excited state than in the ground state. Rotational motions of small molecules in fluid solution are rapid, typically occurring on a timescale of 40 ps or less. The relatively long timescale of fluorescence allows ample time for the solvent molecules to reorient around the excited-state dipole, which lowers its energy and shifts the emission to longer wavelengths. This process is called solvent relaxation and occurs within 10^{-10} s in fluid solution (Figure 1.14). It is these differences between absorption and emission that result in the high sensitivity of emission spectra to solvent polarity, and the smaller spectral changes seen in absorption spectra. Solvent relaxation can result in substantial Stokes shifts. In proteins, tryptophan residues absorb light at 280 nm, and their fluorescence emission occurs near 350 nm.

1.5. FLUORESCENCE ANISOTROPY

Anisotropy measurements are commonly used in the biochemical applications of fluorescence. Anisotropy measurements provide information on the size and shape of proteins or the rigidity of various molecular environments. Anisotropy measurements have been used to measure protein–protein associations, fluidity of membranes, and for immunoassays of numerous substances.

Anisotropy measurements are based on the principle of photoselective excitation of fluorophores by polarized light. Fluorophores preferentially absorb photons whose electric vectors are aligned parallel to the transition moment of the fluorophore. The transition moment has a defined orientation with respect to the molecular axis. In an isotropic solution, the fluorophores are oriented randomly. Upon excitation with polarized light, one selectively excites those fluorophore molecules whose absorption transition dipole is parallel to the electric vector of the excitation (Figure 1.15). This selective excitation results in a partially oriented population of fluorophores (photoselection), and in partially polarized fluorescence emission. Emission also occurs with the light polarized along a fixed axis in the fluorophore. The relative angle between these moments determines the maximum measured anisotropy [r_0, see eq. 10.19]. The fluorescence anisotropy (r) and polarization (P) are defined by

$$r = \frac{I_{\parallel} - I_{\perp}}{I_{\parallel} + 2I_{\perp}} \tag{1.8}$$

$$P = \frac{I_{\parallel} - I_{\perp}}{I_{\parallel} + I_{\perp}} \tag{1.9}$$

where $I_{\parallel}$ and $I_{\perp}$ are the fluorescence intensities of the vertically ($\parallel$) and horizontally ($\perp$) polarized emission, when the sample is excited with vertically polarized light. Anisotropy and polarization are both expressions for the same phenomenon, and these values can be interchanged using eqs. 10.3 and 10.4.

Several phenomena can decrease the measured anisotropy to values lower than the maximum theoretical values. The most common cause is rotational diffusion (Figure 1.15). Such diffusion occurs during the lifetime of the excited state and displaces the emission dipole of the fluorophore. Measurement of this parameter provides information about the relative angular displacement of the fluorophore between the times of absorption and emission. In fluid solution most fluorophores rotate extensively in 50 to 100 ps. Hence, the molecules can rotate many times during the 1–10 ns excited-state lifetime, and the orientation of the polarized emission is randomized. For this reason fluorophores in non-viscous solution typically display anisotropies near zero. Transfer of excitation between fluorophores also results in decreased anisotropies.

The effects of rotational diffusion can be decreased if the fluorophore is bound to a macromolecule. For instance, it is known that the rotational correlation time for the protein human serum albumin (HSA) is near 50 ns. Suppose HSA is covalently labeled with a fluorophore whose lifetime is 50 ns. Assuming no other processes result in loss of anisotropy, the expected anisotropy is given by the Perrin equation:[18]

$$r = \frac{r_0}{1 + (\tau/\theta)} \tag{1.10}$$

where r_0 is the anisotropy that would be measured in the absence of rotational diffusion, and θ is the rotational correlation time for the diffusion process. In this case binding of the fluorophore to the protein has slowed the probe's rate of rotational motion. Assuming $r_0 = 0.4$, the anisotropy is expected to be 0.20. Smaller proteins have shorter correla-

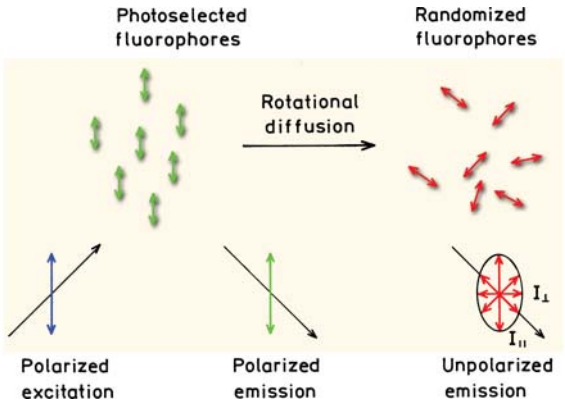

Figure 1.15. Effects of polarized excitation and rotational diffusion on the polarization or anisotropy of the emission.

tion times and are expected to yield lower anisotropies. The anisotropies of larger proteins can also be low if they are labeled with long-lifetime fluorophores. The essential point is that the rotational correlation times for most proteins are comparable to typical fluorescence lifetimes. As a result, measurements of fluorescence anisotropy will be sensitive to any factor that affects the rate of rotational diffusion. The rotational rates of fluorophores in cell membranes also occur on the nanoscale timescale, and the anisotropy values are thus sensitive to membrane composition. For these reasons, measurements of fluorescence polarization are widely used to study the interactions of biological macromolecules.

1.6. RESONANCE ENERGY TRANSFER

Another important process that occurs in the excited state is resonance energy transfer (RET). This process occurs whenever the emission spectrum of a fluorophore, called the donor, overlaps with the absorption spectrum of another molecule, called the acceptor.[19] Such overlap is illustrated in Figure 1.16. The acceptor does not need to be fluorescent. It is important to understand that RET does not involve emission of light by the donor. RET is not the result of emission from the donor being absorbed by the acceptor. Such reabsorption processes are dependent on the overall concentration of the acceptor, and on non-molecular factors such as sample size, and thus are of less interest. There is no intermediate photon in RET. The donor and acceptor are coupled by a dipole–dipole interaction. For these reasons the term RET is preferred over the term fluorescence resonance energy transfer (FRET), which is also in common use.

The extent of energy transfer is determined by the distance between the donor and acceptor, and the extent of spectral overlap. For convenience the spectral overlap (Figure 1.16) is described in terms of the Förster distance (R_0). The rate of energy transfer $k_T(r)$ is given by

$$k_T(r) = \frac{1}{\tau_D}\left(\frac{R_0}{r}\right)^6 \tag{1.11}$$

where r is the distance between the donor (D) and acceptor (A) and τ_D is the lifetime of the donor in the absence of energy transfer. The efficiency of energy transfer for a single donor–acceptor pair at a fixed distance is

$$E = \frac{R_0^6}{R_0^6 + r^6} \tag{1.12}$$

Hence the extent of transfer depends on distance (r). Fortunately, the Förster distances are comparable in size to biological macromolecules: 30 to 60 Å. For this reason energy transfer has been used as a "spectroscopic ruler" for measurements of distance between sites on proteins.[20] The value of R_0 for energy transfer should not be confused with the fundamental anisotropies (r_0).

The field of RET is large and complex. The theory is different for donors and acceptors that are covalently linked, free in solution, or contained in the restricted geometries of membranes or DNA. Additionally, depending on donor lifetime, diffusion can increase the extent of energy transfer beyond that predicted by eq. 1.12.

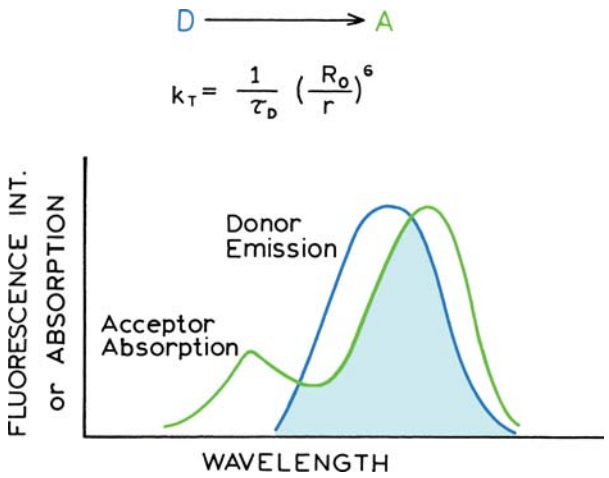

Figure 1.16. Spectral overlap for fluorescence resonance energy transfer (RET).

1.7. STEADY-STATE AND TIME-RESOLVED FLUORESCENCE

Fluorescence measurements can be broadly classified into two types of measurements: steady-state and time-resolved. Steady-state measurements, the most common type, are those performed with constant illumination and observation. The sample is illuminated with a continuous beam of light, and the intensity or emission spectrum is recorded (Figure 1.17). Because of the ns timescale of fluorescence, most measurements are steady-state measurements. When the sample is first exposed to light, steady state is reached almost immediately.

The second type of measurement is time-resolved, which is used for measuring intensity decays or anisotropy decays. For these measurements the sample is exposed to a pulse of light, where the pulse width is typically shorter than the decay time of the sample (Figure 1.17). This intensity decay is recorded with a high-speed detection system that permits the intensity or anisotropy to be measured on the ns timescale.

It is important to understand the relationship between steady-state and time-resolved measurements. A steady-state observation is simply an average of the time-resolved phenomena over the intensity decay of the sample. For instance, consider a fluorophore that displays a single decay time (τ) and a single rotational correlation time (θ). The intensity and anisotropy decays are given by

$$I(t) = I_0\, e^{-t/\tau} \tag{1.13}$$

$$r(t) = r_0\, e^{-t/\theta} \tag{1.14}$$

where I_0 and r_0 are the intensities and anisotropies at $t = 0$, immediately following the excitation pulse, respectively.

Equations 1.13 and 1.14 can be used to illustrate how the decay time determines what can be observed using fluorescence. The steady-state anisotropy (r) is given by the average of $r(t)$ weighted by $I(t)$:

$$r = \frac{\int_0^\infty r(t)I(t)\,dt}{\int_0^\infty I(t)\,dt} \tag{1.15}$$

In this equation the denominator is present to normalize the anisotropy to be independent of total intensity. In the numerator the anisotropy at any time t contributes to the steady-state anisotropy according to the intensity at time t.

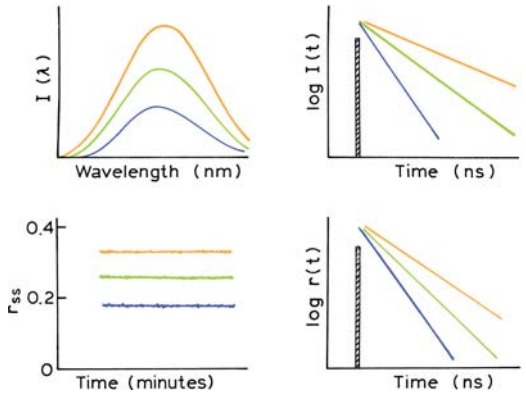

Figure 1.17. Comparison of steady-state and time-resolved fluorescence spectroscopy.

Substitution of eqs. 1.13 and 1.14 into 1.15 yields the Perrin equation, 1.10.

Perhaps a simpler example is how the steady-state intensity (I_{SS}) is related to the decay time. The steady-state intensity is given by

$$I_{SS} = \int_0^\infty I_0\, e^{-t/\tau}\, dt = I_0\tau \tag{1.16}$$

The value of I_0 can be considered to be a parameter that depends on the fluorophore concentration and a number of instrumental parameters. Hence, in molecular terms, the steady-state intensity is proportional to the lifetime. This makes sense in consideration of eqs. 1.1 and 1.2, which showed that the quantum yield is proportional to the lifetime.

1.7.1. Why Time-Resolved Measurements?

While steady-state fluorescence measurements are simple, nanosecond time-resolved measurements typically require complex and expensive instrumentation. Given the relationship between steady-state and time-resolved measurements, what is the value of these more complex measurements? It turns out that much of the molecular information available from fluorescence is lost during the time averaging process. For example, anisotropy decays of fluorescent macromolecules are frequently more complex than a single exponential (eq. 1.14). The precise shape of the anisotropy decay contains information about the shape of the macromolecule and its flexibility. Unfortunately, this shape information is lost during averaging of the anisotropy over the decay time (eq. 1.15). Irrespective of the form of $r(t)$, eq. 1.15 yields a

single steady-state anisotropy. In principle, the value of r still reflects the anisotropy decay and shape of the molecule. In practice, the information from r alone is not sufficient to reveal the form of $r(t)$ or the shape of the molecule.

The intensity decays also contain information that is lost during the averaging process. Frequently, macromolecules can exist in more than a single conformation, and the decay time of a bound probe may depend on conformation. The intensity decay could reveal two decay times, and thus the presence of more than one conformational state. The steady-state intensity will only reveal an average intensity dependent on a weighted averaged of the two decay times.

There are numerous additional reasons for measuring time-resolved fluorescence. In the presence of energy transfer, the intensity decays reveal how acceptors are distributed in space around the donors. Time-resolved measurements reveal whether quenching is due to diffusion or to complex formation with the ground-state fluorophores. In fluorescence, much of the molecular information content is available only by time-resolved measurements.

1.8. BIOCHEMICAL FLUOROPHORES

Fluorophores are divided into two general classes—intrinsic and extrinsic. Intrinsic fluorophores are those that occur naturally. Extrinsic fluorophores are those added to a sample that does not display the desired spectral properties. In proteins, the dominant fluorophore is the indole group of tryptophan (Figure 1.18). Indole absorbs near 280 nm, and emits near 340 nm. The emission spectrum of indole is highly sensitive to solvent polarity. The emission of indole may be blue shifted if the group is buried within a native protein (N), and its emission may shift to longer wavelengths (red shift) when the protein is unfolded (U).

Membranes typically do not display intrinsic fluorescence. For this reason it is common to label membranes with probes which spontaneously partition into the nonpolar side chain region of the membranes. One of the most commonly used membrane probes is diphenylhexatriene (DPH). Because of its low solubility and quenched emission in water, DPH emission is only seen from membrane-bound DPH (Figure 1.18). Other lipid probes include fluorophores attached to lipid or fatty acid chains.

While DNA contains nitrogenous bases that look like fluorophores, DNA is weakly or nonfluorescent. However, a wide variety of dyes bind spontaneously to DNA—such as acridines, ethidium bromide, and other planar cationic species. For this reason staining of cells with dyes that bind to DNA is widely used to visualize and identify chromosomes. One example of a commonly used DNA probe is 4',6-diamidino-2-phenolindole (DAPI). There is a wide variety of fluorophores that spontaneously bind to DNA.

A great variety of other substances display significant fluorescence. Among biological molecules, one can observe fluorescence from reduced nicotinamide adenine dinucleotide (NADH), from oxidized flavins (FAD, the adenine dinucleotide, and FMN, the mononucleotide), and pyridoxyl phosphate, as well as from chlorophyll. Occasionally, a species of interest is not fluorescent, or is not fluorescent in a convenient region of the UV visible spectrum. A wide variety of extrinsic probes have been developed for labeling the macromolecules in such cases. Two of the most widely used probes, dansyl chloride DNS-Cl, which stands for 1-dimethylamino-5-naphthylsulfonyl chloride, and fluorescein isothiocyanate (FITC), are shown in Figure 1.19. These probes react with the free amino groups of proteins, resulting in proteins that fluoresce at blue (DNS) or green (FITC) wavelengths.

Proteins can also be labeled on free sulfhydryl groups using maleimide reagents such as Bodipi 499/508 maleimide. It is frequently useful to use longer-wavelength probes such as the rhodamine dye Texas Red. Cyanine dyes are frequently used for labeling nucleic acids, as shown for the labeled nucleotide Cy3-4-dUTP. A useful fluorescent probe is one that displays a high intensity, is stable during continued illumination, and does not substantially perturb the biomolecule or process being studied.

1.8.1. Fluorescent Indicators

Another class of fluorophores consists of the fluorescent indicators. These are fluorophores whose spectral properties are sensitive to a substance of interest. One example is Sodium Green, which is shown in Figure 1.20. This fluorophore contains a central azacrown ether, which binds Na^+. Upon binding of sodium the emission intensity of Sodium Green increases, allowing the amount of Na^+ to be determined. Fluorescent indicators are presently available for a variety of substances, including Ca^{2+}, Mg^{2+}, Na^+, Cl^-, and O_2, as well as pH. The applications of fluorescence to chemical sensing is described in Chapter 19.

1.9. MOLECULAR INFORMATION FROM FLUORESCENCE

1.9.1. Emission Spectra and the Stokes Shift

The most dramatic aspect of fluorescence is its occurrence at wavelengths longer than those at which absorption occurs. These Stokes shifts, which are most dramatic for

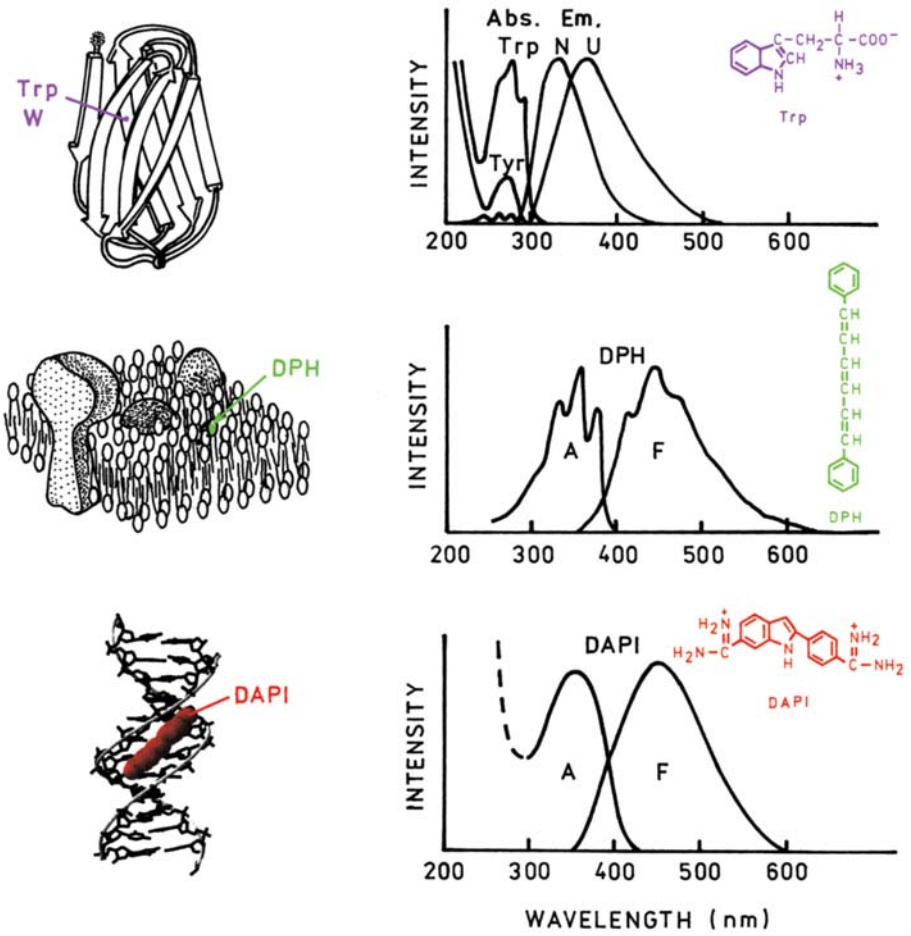

Figure 1.18. Absorption and emission spectra of biomolecules. Top, tryptophan emission from proteins. Middle, spectra of extrinsic membrane probe DPH. Bottom, spectra of the DAPI bound to DNA (– – –). DNA itself displays very weak emission. Reprinted with permission by Wiley-VCH, STM. From [21].

polar fluorophores in polar solvents, are due to interactions between the fluorophore and its immediate environment. The indole group of tryptophan residues in proteins is one such solvent-sensitive fluorophore, and the emission spectra of indole can reveal the location of tryptophan residues in proteins. The emission from an exposed surface residue will occur at longer wavelengths than that from a tryptophan residue in the protein's interior. This phenomenon was illustrated in the top part of Figure 1.18, which shows a shift in the spectrum of a tryptophan residue upon unfolding of a protein and the subsequent exposure of the tryptophan residue to the aqueous phase. Prior to unfolding, the residue is shielded from the solvent by the folded protein.

A valuable property of many fluorophores is their sensitivity to the surrounding environment. The emission spectra and intensities of extrinsic probes are often used to determine a probe's location on a macromolecule. For example, one of the widely used probes for such studies is 6-(p-toluidinyl)naphthalene-2-sulfonate (TNS), which displays the favorable property of being very weakly fluorescent in water (Figure 1.21). The green emission of TNS in the absence of protein is barely visible in the photographs. Weak fluorescence in water and strong fluorescence when bound to a biomolecule is a convenient property shared by other widely used probes, including many DNA stains. The protein apomyoglobin contains a hydrophobic pocket that binds the heme group. This pocket can also bind other nonpolar molecules. Upon the addition of apomyoglobin to a solution of TNS, there is a large increase in fluorescence intensity, as well as a shift of the emission spectrum to shorter wavelengths. This increase in TNS fluorescence reflects the nonpolar character of the heme-binding site of apomyoglobin. TNS also binds to membranes (Figure 1.21). The emission spectrum of TNS when bound to model membranes of dimyristoyl-L-α-phosphatidylcholine (DMPC) is somewhat weaker and at longer wavelengths

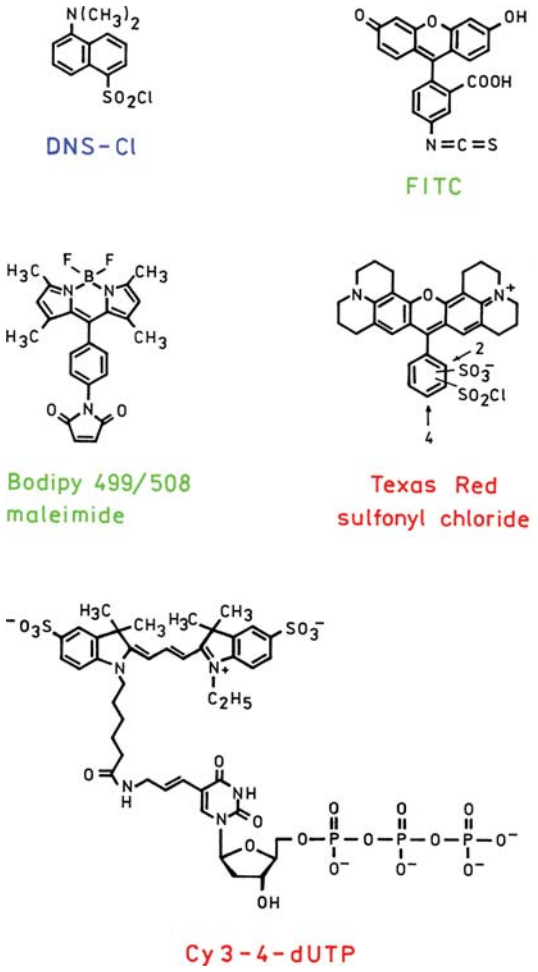

Figure 1.19. Fluorophores for covalent labeling of biomolecules.

compared to that of apomyoglobin. This indicates that the TNS binding sites on the surface of the membrane are more polar. From the emission spectrum it appears that TNS binds to the polar head group region of the membranes, rather than to the nonpolar acyl side chain region. Hence, the emission spectra of solvent-sensitive fluorophores provide information on the location of the binding sites on the macromolecules.

1.9.2. Quenching of Fluorescence

As described in Section 1.4.1, a wide variety of small molecules or ions can act as quenchers of fluorescence, that is, they decrease the intensity of the emission. These substances include iodide (I^-), oxygen, and acrylamide. The accessibility of fluorophores to such quenchers can be used to determine the location of probes on macromolecules, or the porosity of proteins and membranes to quenchers. This

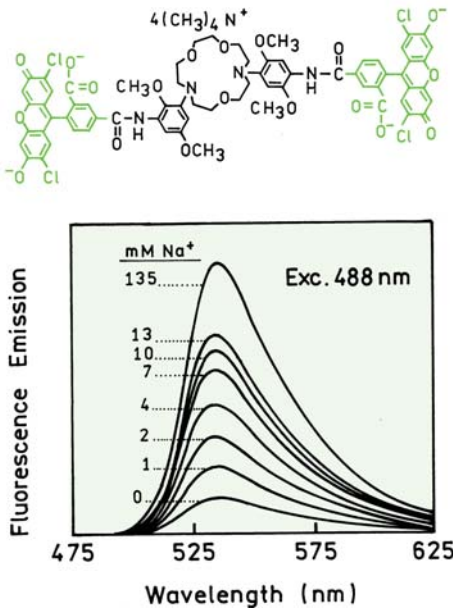

Figure 1.20. Effects of sodium on the emission of Sodium Green. From [22].

concept is illustrated in Figure 1.22, which shows the emission intensity of a protein- or membrane-bound fluorophore in the presence of the water-soluble quencher iodide, I^-. As shown on the right-hand side of the figure, the emission intensity of a tryptophan on the protein's surface (W_2), or on the surface of a cell membrane (P_2, right), will be decreased in the presence of a water-soluble quencher. The intensity of a buried tryptophan residue (W_1) or of a probe in the membrane interior (P_1) will be less affected by the dissolved iodide (left). The iodide Stern-Volmer quenching constant K in eq. 1.6 will be larger for the exposed fluorophores than for the buried fluorophores. Alternatively, one can add lipid-soluble quenchers, such as brominated fatty acids, to study the interior acyl side chain region of membranes, by measurement from the extent of quenching by the lipid-soluble quencher.

1.9.3. Fluorescence Polarization or Anisotropy

As described in Section 1.5, fluorophores absorb light along a particular direction with respect to the molecular axes. For example, DPH only absorbs light polarized along its long axis (Figure 1.18). The extent to which a fluorophore rotates during the excited-state lifetime determines its polarization or anisotropy. The phenomenon of fluorescence polarization can be used to measure the apparent vol-

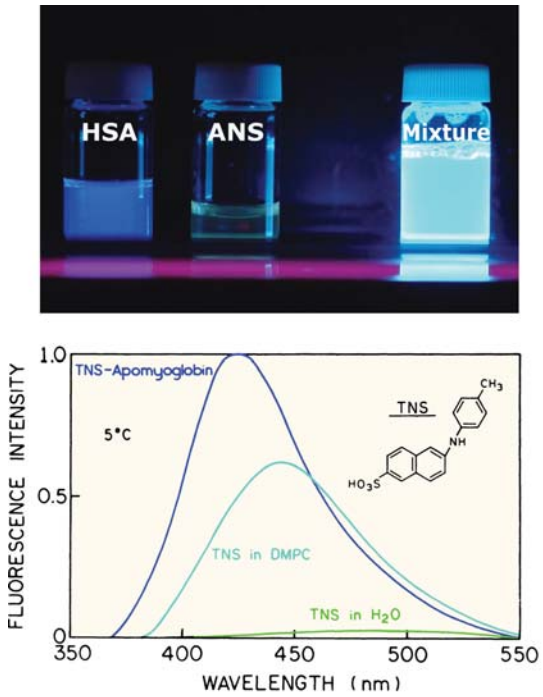

Figure 1.21. Emission spectra of TNS in water, bound to apomyoglobin, and bound to lipid vesicles.

ume (or molecular weight) of proteins. This measurement is possible because larger proteins rotate more slowly. Hence, if a protein binds to another protein, the rotational rate decreases, and the anisotropy(s) increases (Figure 1.23). The rotational rate of a molecule is often described by its rotational correlation time θ, which is related to

$$\theta = \frac{\eta V}{RT} \tag{1.17}$$

where η is the viscosity, V is the molecular volume, R is the gas constant, and T is the temperature in °K. Suppose a protein is labeled with DNS-Cl (Figure 1.23). If the protein associates with another protein, the volume increases and so does the rotational correlation time. This causes the anisotropy to increase because of the relationship between the steady-state anisotropy r to the rotational correlation time θ (eq. 1.10).

Fluorescence polarization measurements have also been used to determine the apparent viscosity of the side chain region (center) of membranes. Such measurements of microviscosity are typically performed using a hydrophobic probe like DPH (Figure 1.23), which partitions into the membrane. The viscosity of membranes is known to decrease in the presence of unsaturated fatty acid side

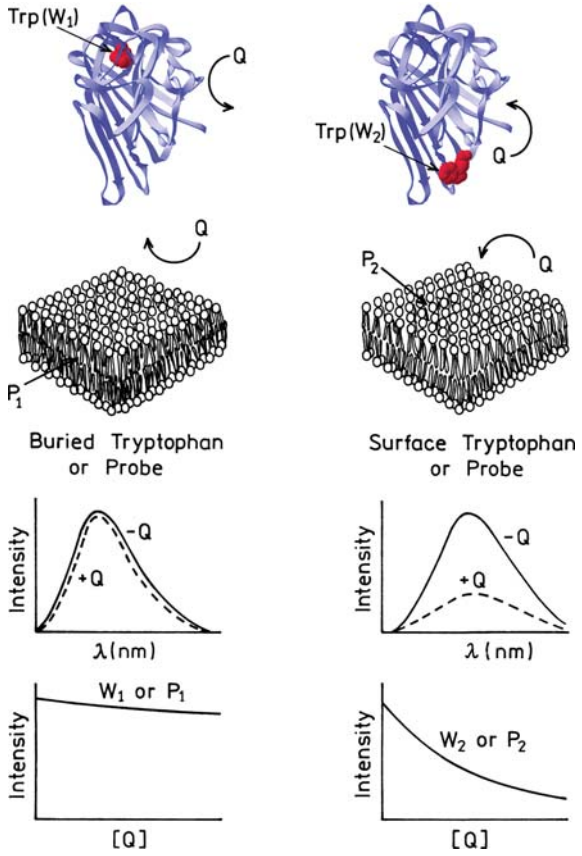

Figure 1.22. Accessibility of fluorophores to the quencher (Q). Reprinted with permission by Wiley-VCH, STM. From [21].

chains. Hence, an increase in the amount of unsaturated fatty acid is expected to decrease the anisotropy. The apparent microviscosity of the membrane is determined by comparing the polarization of the probe measured in the membrane with that observed in solutions of known viscosity.

Anisotropy measurements are widely used in biochemistry, and are even used for clinical immunoassays. One reason for this usage is the ease with which these absolute values can be measured and compared between laboratories.

1.9.4. Resonance Energy Transfer

Resonance energy transfer (RET), sometimes called fluorescence resonance energy transfer (FRET), provides an opportunity to measure the distances between sites on macromolecules. Förster distances are typically in the range of 15 to 60 Å, which is comparable to the diameter of many proteins and to the thickness of membranes. According to eq. 1.12, the distance between a donor and acceptor can be calculated from the transfer efficiency.

The use of RET to measure protein association and distance is shown in Figure 1.24 for two monomers that associate to form a dimer. Suppose one monomer contains a tryptophan residue, and the other a dansyl group. The Förster distance is determined by the spectral overlap of the trp donor emission with the dansyl acceptor absorption. Upon association RET will occur, which decreases the intensity of the donor emission (Figure 1.24). The extent of donor quenching can be used to calculate the donor-to-acceptor distance in the dimer (eq. 1.12). It is also important to notice that RET provides a method to measure protein association because it occurs whenever the donor and acceptor are within the Förster distance.

1.10. BIOCHEMICAL EXAMPLES OF BASIC PHENOMENA

The uses of fluorescence in biochemistry can be illustrated by several simple examples. The emission spectra of proteins are often sensitive to protein structure. This sensitivity is illustrated by melittin,[23] which is a 26-amino-acid peptide containing a single tryptophan residue. Depending upon the solution conditions, melittin can exist as a monomer or self-associate to form a tetramer. When this occurs the tryptophan emission maximum shifts to shorter wavelengths (Figure 1.25). These spectra show that a protein association reaction can be followed in dilute solution using simple measurements of the emission spectra.

Association reactions can also be followed by anisotropy measurements. Figure 1.26 shows anisotropy measurements of melittin upon addition of calmodulin.[24] Calmodulin does not contain any tryptophan, so the total tryptophan emission is only due to melittin. Upon addition of calmodulin the melittin anisotropy increases about twofold. This effect is due to slower rotational diffusion of the melittin–calmodulin complex as compared to melittin alone. The emission spectra of melittin show that the tryptophan residue becomes shielded from the solvent upon binding to calmodulin. The tryptophan residue is probably located at the interface between the two proteins.

Resonance energy transfer can also be used to study DNA hybridization.[25] Figure 1.27 shows complementary DNA oligomers labeled with either fluorescein (Fl) or rhodamine (Rh). Hybridization results in increased RET from fluorescein to rhodamine, and decreased fluorescein intensities (lower panel). Disassociation of the oligomers results in less RET and increased fluorescein intensities. The extent of hybridization can be followed by simple intensity measurements.

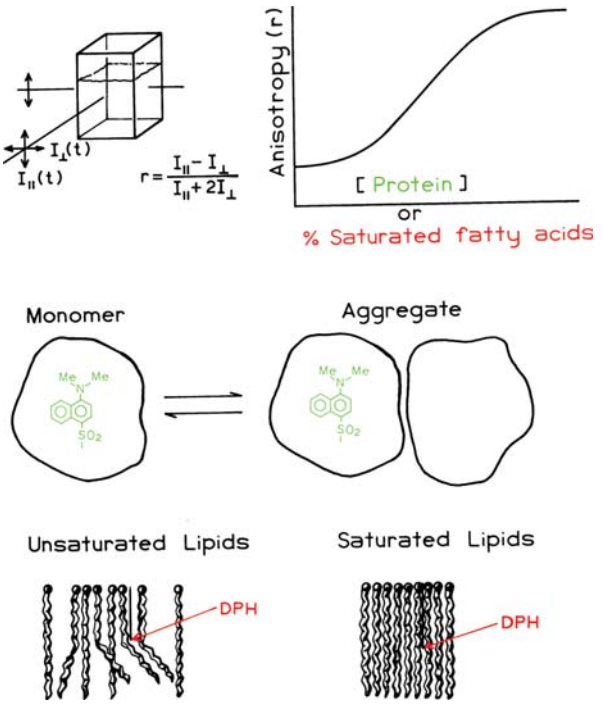

Figure 1.23. Effect of protein association and membrane microviscosity on the fluorescence anisotropy. From [21].

RET can also be used to study gene expression. One approach is to use donor- and acceptor-labeled DNA oligomers (Figure 1.28). If a complementary mRNA is present, the oligomers can bind close to each other.[26] The RET will result in increased emission intensity from the acceptor. The lower panels show fluorescence microscopy images of human dermal fibroblasts. The cells on the left were not stimulated and did not produce the K-ras gene product. The cells on the right were stimulated to cause expression of the K-ras oncogene. Mutations in the gene are associated with human colorectal cancer.[27] The images show the emission intensity of the acceptor. Significant acceptor intensity is only found in the stimulated cells where the mRNA for K-ras is present. RET is now widely used in cellular imaging to detect many types of gene expression and the intracellular proximity of biomolecules.

1.11. NEW FLUORESCENCE TECHNOLOGIES

1.11.1. Multiphoton Excitation

During the past several years technological advances have provided new uses of fluorescence. These technologies have been quickly adopted and are becoming mainstream methods. One of these technologies is two-photon or multi-

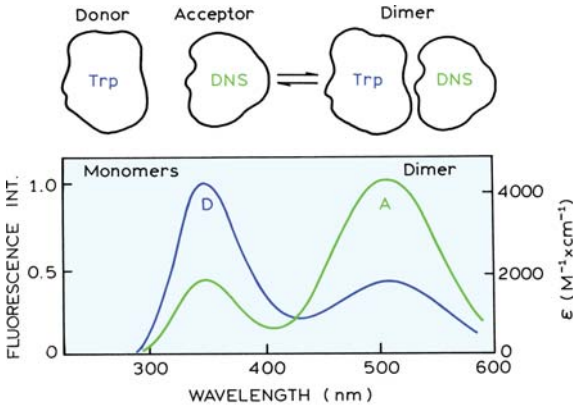

Figure 1.24. Energy transfer between donor- (D) and acceptor- (A) labeled monomers, which associate to form a dimer. In this case the donor is tryptophan and the acceptor DNS.

photon excitation and multiphoton microscopy.[28–30] Fluorescence is usually excited by absorption of a single photon with a wavelength within the absorption band of the fluorophore. Pulse lasers with femtosecond pulse widths can excite fluorophores by two-photon absorption. Such lasers have become easy to use and available with microscopes. If the laser intensity is high, a fluorophore can simultaneously absorb two long-wavelength photons to reach the first singlet state (Figure 1.29). This process depends strongly on the light intensity and occurs only at the focal point of the laser beam. This can be seen in the photo, where emission is occurring only from a single spot within the sample. Fluorophores outside the focal volume are not excited.

Localized excitation from two-photon excitation has found widespread use in fluorescence microscopy. Multiphoton excitations allow imaging from only the focal plane of a microscope. This is an advantage because fluorescence

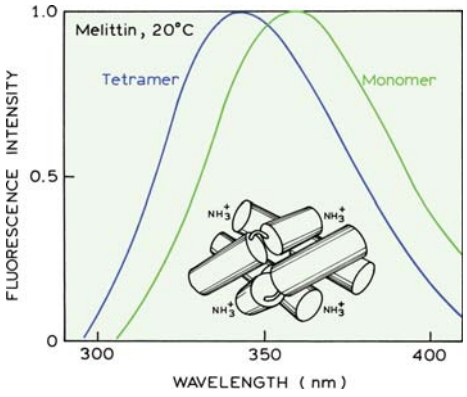

Figure 1.25. Emission spectra of melittin monomer and tetramer. Excitation was at 295 nm. In the schematic structure, the tryptophans are located in the center between the four helices. From [23].

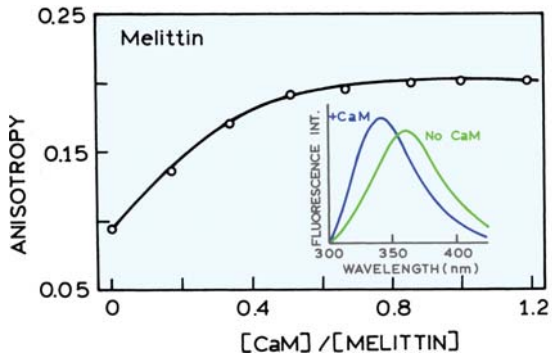

Figure 1.26. Effect of melittin–calmodulin association on the anisotropy of melittin. **Inset**: Emission spectra of melittin in the presence and absence of calmodulin (CaM). Modified from [24].

images are otherwise distorted from fluorescence from above and below the focal plane. Figure 1.30 shows an example of the remarkably sharp images obtainable with multiphoton excitation. The cells were labeled with three probes: DAPI for DNA, Patman for membranes, and tetramethylrhodamine for mitochondria. A single excitation wavelength of 780 nm was used. This wavelength does not excite any of the fluorophores by one-photon absorption, but 780 nm is absorbed by all these fluorophores through a multiphoton process. The images are sharp because there is no actual phase fluorescence that decreases the contrast in non-confocal fluorescence microscopy. Such images are now being obtained in many laboratories.

1.11.2. Fluorescence Correlation Spectroscopy

Fluorescence correlation spectroscopy (FCS) has rapidly become a widely used tool to study a wide range of association reactions.[31] FCS is based on the temporal fluctuations occurring in a small observed volume. Femtoliter volumes can be obtained with localized multiphoton excitation or using confocal optics (Figure 1.31, top). Bursts of photons are seen as single fluorophores diffuse in and out of the laser beam. The method is highly sensitive since only a few fluorophores are observed at one time. In fact, FCS cannot be performed if the solution is too concentrated and there are many fluorophores in the observed volume. Less fluorophores result in more fluctuations, and more fluorophores result in smaller fluctuations and a more constant average signal.

FCS is performed by observing the intensity fluctuations with time (Figure 1.31, middle panel). The rate of fluctuation depends on the rate of fluorophore diffusion. The intensity increases and decreases more rapidly if the

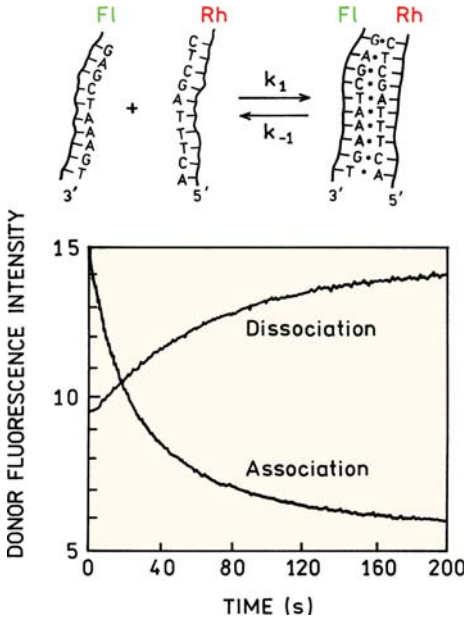

Figure 1.27. DNA hybridization measured by RET between fluorescein (Fl) and rhodamine (Rh). The lower panel shows the fluorescein donor intensities. Revised from [25].

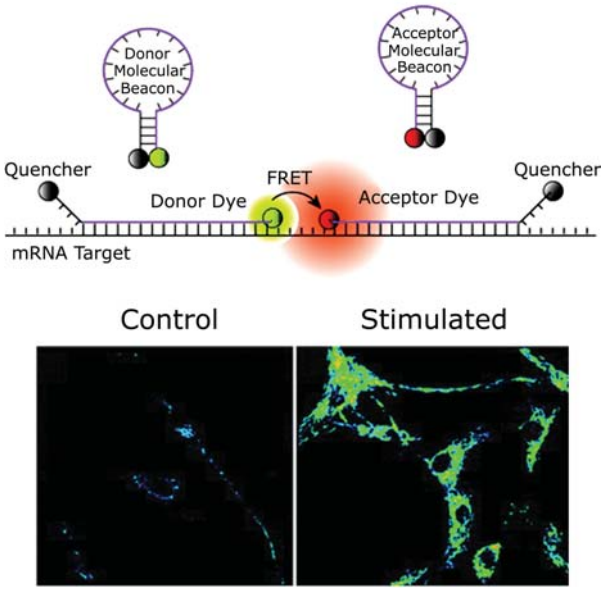

Figure 1.28. Detection of mRNA with RET and molecular beacons. The lower panels show acceptor intensity images of control cells and stimulated fibroblasts expressing the K-ras gene. Revised from [26].

fluorophores diffuse rapidly. If the fluorophores diffuse slowly they remain in the observed volume for a longer period of time and the intensity fluctuations occur more slowly. The amplitude and speed of the fluctuations are used to calculate the correlation function (lower panel). The height of the curve is inversely proportional to the average number of fluorophores being observed. The position of the curve on the time axis indicates the fluorophore's diffusion coefficient.

Figure 1.32 shows how FCS can be used to study ligand bindings to a single neuronal cell. The ligand was an Alexa-labeled benzodiazepine.[32] Benzodiazepines are used to treat anxiety and other disorders. FCS curves are shown for Alexa-Bz in solution and when bound to its receptor. The receptors were present on the membrane of a single neuronal cell where the laser beam was focused. The FCS curve clearly shows binding of Alexa-Bz to the receptor by a 50-fold increase in the diffusion time. Such measurements can be performed rapidly with high sensitivity. FCS will be used increasingly in drug discovery and biotechnology, as well as biochemistry and biophysics.

1.11.3. Single-Molecule Detection

Observations on single molecules represent the highest obtainable sensitivity. Single-molecule detection (SMD) is now being performed in many laboratories.[33–34] At present

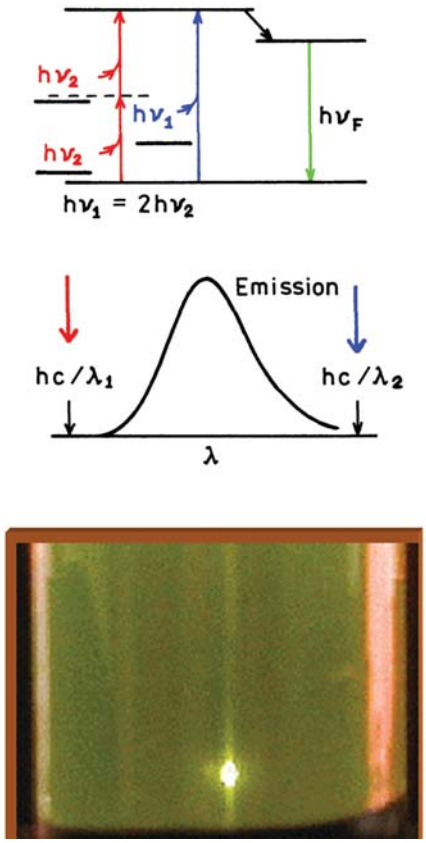

Figure 1.29. Jablonski diagram for two-photon excitation. The photo shows localized excitation at the focal point of the laser beam.

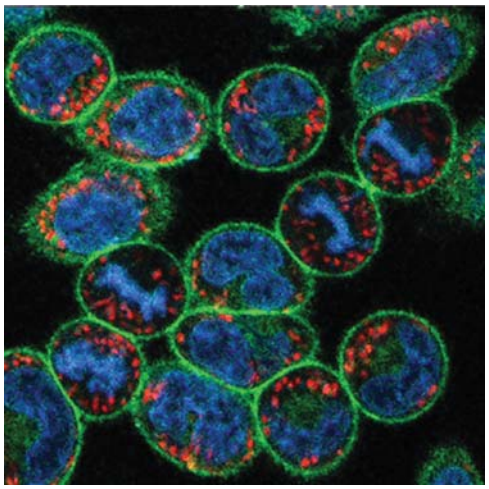

Figure 1.30. Fluorescence image of RBL-3H3 cells stained with DAPI (blue), Patman (green), and tetramethylrhodamine (red). Courtesy of Dr. W. Zipfel and Dr. W. Webb, Cornell University. Reprinted with permission from [30].

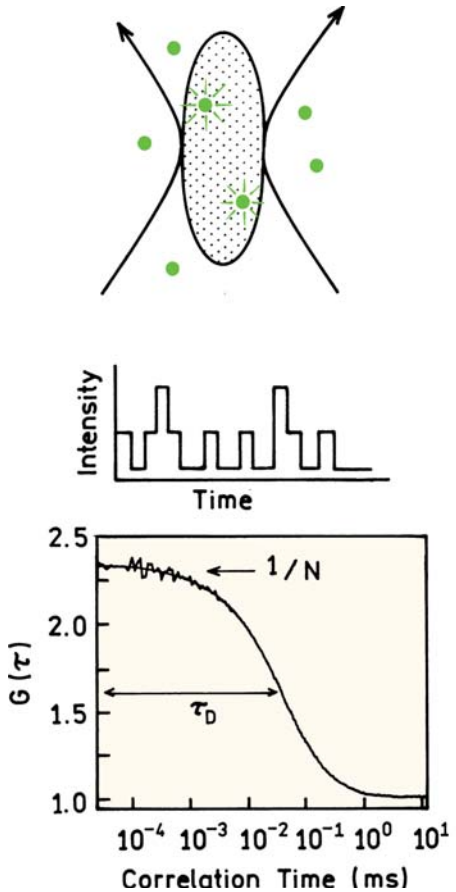

Figure 1.31. Fluorescence correlation spectroscopy. **Top**: observed volume shown as a shaded area. **Middle**: intensity fluctuations. **Bottom**: correlation function.

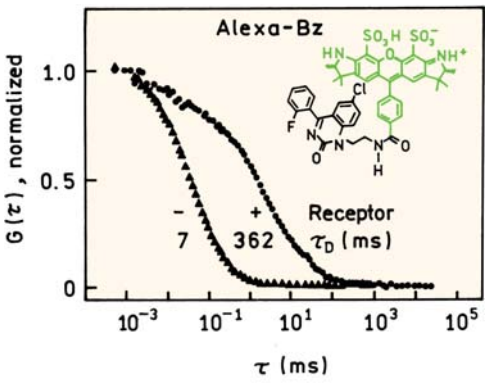

Figure 1.32. FCS of an Alexa-labeled benzodiazepine (Alexa-Bz) in solution and on a single neuronal cell. Revised from [32].

most single-molecule experiments are performed on immobilized fluorophores, with fluorophores chosen for their high quantum yields and photostability (Chapter 23). A typical instrument for SMD consists of laser excitation through microscope objective, a scanning stage to move the sample and confocal optics to reject unwanted signals. SMD is now being extended to include UV-absorbing fluorophores, which was considered unlikely just a short time ago. The probe 2,2'-dimethyl-p-quaterphenyl (DMQ) has an absorption maximum of 275 nm and an emission maximum of 350 nm. Figure 1.33 (left) shows intensity images of DMQ on a quartz cover slip.[35] The spots represent the individual DMQ molecules, which can yield signals as high as 70,000 photons per second. The technology for SMD has advanced so rapidly that the lifetimes of single molecules can also be measured at the same time the intensity images are being collected (right). The individual DMQ molecules all display lifetimes near 1.1 ns.

Without the use of SMD, almost all experiments observe a large number of molecules. These measurements reveal the ensemble average of the measured properties. When observing a single molecule there is no ensemble averaging, allowing for the behavior of a single molecule to be studied. Such an experiment is shown in Figure 1.34 for a hairpin ribozyme labeled with a donor and acceptor. Steady-state measurements on a solution of the labeled ribozyme would yield the average amount of energy transfer, but would not reveal the presence of subpopulations showing different amounts of energy transfer. Single-molecule experiments show that an individual ribozyme molecule fluctuates between conformations with lower or higher amounts of energy transfer.[36] These conformational changes are seen from simultaneous increases and decreas-

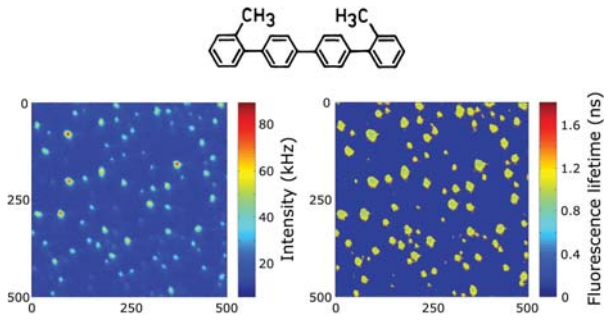

Figure 1.33. Single-molecule intensities and lifetimes of DMQ in a quartz slide. Excitation at 266 nm. Figure courtesy of Dr. S. Seeger, University of Zürich. Reprinted with permission from [35].

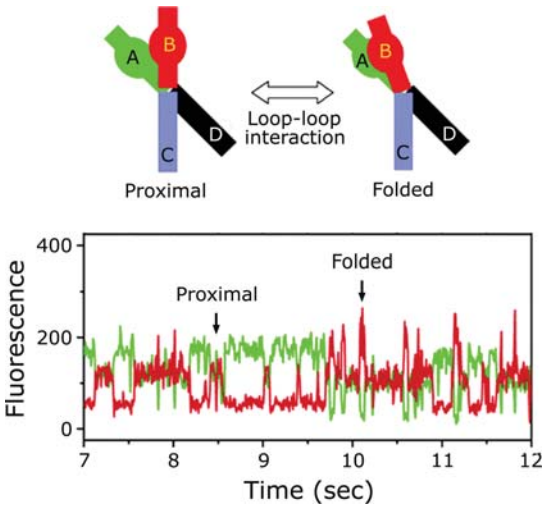

Figure 1.34. Single-molecule RET between a donor (green) and acceptor (red) on a hairpin ribozyme. Revised from [36].

es in donor and acceptor emission. The single-molecule experiments also reveal the rate of the conformational changes. Such detailed information is not available from ensemble measurements.

At present single-molecule experiments are mostly performed using cleaned surfaces to minimize background. However, SMD can be extended to intracellular molecules if they are not diffusing too rapidly. One such experiment is detection of single molecules of the oncogen product Ras within cells.[37] Ras was labeled with yellow fluorescent protein (YFP). Upon activation Ras binds GTP (Figure 1.35). In this experiment activated Ras binds GTP labeled with a fluorophore called Bodipy TR. Single molecules of YFP-Ras were imaged on a plasma membrane (lower left). Upon activation of Ras, fluorescent red spots appeared that were

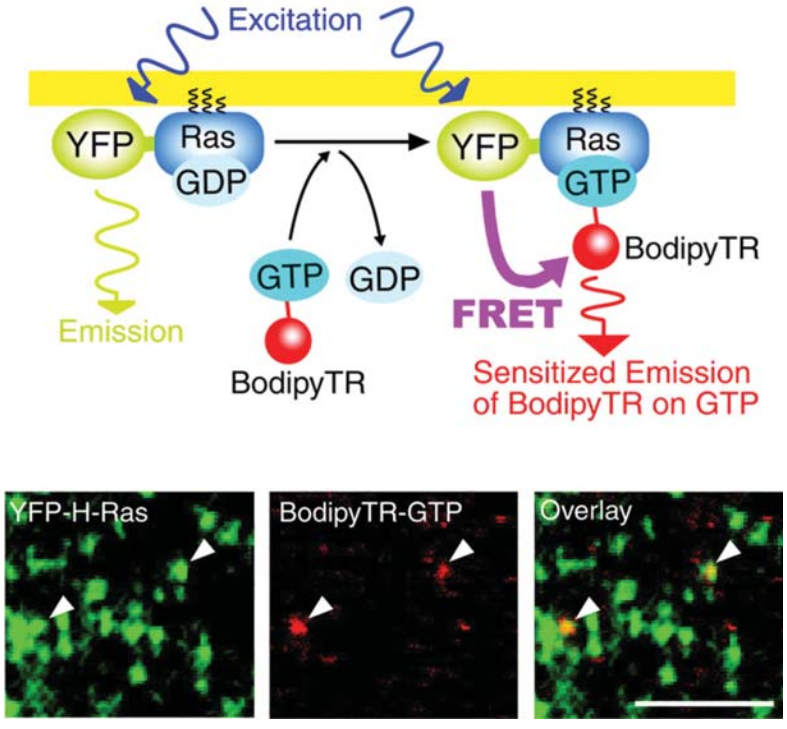

Figure 1.35. Binding of Bodipy TR-labeled GTP to activated YFP-Ras. The lower panels show single-molecule images of YFP-Ras and Bodipy TR-labeled GTP. The overlay of both images shows the location of activated Ras from the plasma membrane of KB cells. Bar = 5 μm. Revised from [37].

due to binding of Bodipy TR-GTP. The regions where emission from both YFP and Bodipy TR is observed corresponds to single copies of the activated Ras protein.

1.12. OVERVIEW OF FLUORESCENCE SPECTROSCOPY

Fluorescence spectroscopy can be applied to a wide range of problems in the chemical and biological sciences. The measurements can provide information on a wide range of molecular processes, including the interactions of solvent molecules with fluorophores, rotational diffusion of biomolecules, distances between sites on biomolecules, conformational changes, and binding interactions. The usefulness of fluorescence is being expanded by advances in technology for cellular imaging and single-molecule detection. These advances in fluorescence technology are decreasing the cost and complexity of previously complex instruments. Fluorescence spectroscopy will continue to contribute to rapid advances in biology, biotechnology and nanotechnology.

REFERENCES

1. Herschel, Sir JFW. 1845. On a case of superficial colour presented by a homogeneous liquid internally colourless. *Phil Trans Roy Soc (London)* **135**:143–145.
2. Gillispie CC, ed. 1972. John Frederick William Herschel. In *Dictionary of scientific biography*, Vol. 6, pp. 323–328. Charles Scribner's Sons, New York.
3. Undenfriend S. 1995. Development of the spectrophotofluorometer and its commercialization. *Protein Sci* **4**:542–551.
4. Martin BR, Richardson F. 1979. Lanthanides as probes for calcium in biological systems, *Quart Rev Biophys* **12**:181–203.
5. Berlman IB. 1971. *Handbook of fluorescence spectra of aromatic molecules*, 2nd ed. Academic Press, New York.
6. Jablonski A. 1935. Über den Mechanisms des Photolumineszenz von Farbstoffphosphoren, *Z Phys* **94**:38–46.
7. Szudy J, ed. 1998. *Born 100 years ago: Aleksander Jablonski (1898–1980)*, Uniwersytet Mikolaja Kopernika, Torun, Poland.
8. Acta Physica Polonica. 1978. Polska Akademia Nauk Instytut Fizyki. *Europhys J*, Vol. A65(6).
9. Stokes GG. 1852. On the change of refrangibility of light. *Phil Trans R Soc (London)* **142**:463–562.
10. Kasha M. 1950. Characterization of electronic transitions in complex molecules. *Disc Faraday Soc* **9**:14–19.
11. Courtesy of Dr. Ignacy Gryczynski.
12. Birks JB. 1970. *Photophysics of aromatic molecules*. John Wiley & Sons, New York.
13. Lakowicz JR, Balter A. 1982. Analysis of excited state processes by phase-modulation fluorescence spectroscopy. *Biophys Chem* **16**:117–132.
14. Photo courtesy of Dr. Ignacy Gryczynski and Dr. Zygmunt Gryczynski.
15. Birks JB. 1973. *Organic molecular photophysics*. John Wiley & Sons, New York.
16. Strickler SJ, Berg RA. 1962. Relationship between absorption intensity and fluorescence lifetime of molecules. *J Chem Phys* **37**(4):814–822.
17. See [12], p. 120.
18. Berberan-Santos MN. 2001. Pioneering contributions of Jean and Francis Perrin to molecular luminescence. In *New trends in fluorescence spectroscopy: applications to chemical and life sciences*, Vol. 18, pp. 7–33. Ed B Valeur, J-C Brochon. Springer, New York.
19. Förster Th. 1948. Intermolecular energy migration and fluorescence (Transl RS Knox). *Ann Phys (Leipzig)* **2**:55–75.
20. Stryer L. 1978. Fluorescence energy transfer as a spectroscopic ruler. *Annu Rev Biochem* **47**:819–846.
21. Lakowicz JR. 1995. Fluorescence spectroscopy of biomolecules. In *Encyclopedia of molecular biology and molecular medicine*, pp. 294–306. Ed RA Meyers. VCH Publishers, New York.
22. Haugland RP. 2002. LIVE/DEAD BacLight bacterial viability kits. In *Handbook of fluorescent probes and research products*, 9th ed., pp. 626–628. Ed J Gregory. Molecular Probes, Eugene, OR.
23. Gryczynski I, Lakowicz JR. Unpublished observations.
24. Lakowicz JR, Gryczynski I, Laczko G, Wiczk W, Johnson ML. 1994. Distribution of distances between the tryptophan and the N-terminal residue of melittin in its complex with calmodulin, troponin, C, and phospholipids. *Protein Sci* **3**:628–637.
25. Morrison LE, Stols LM. 1993. Sensitive fluorescence-based thermodynamic and kinetic measurements of DNA hybridization in solution. *Biochemistry* **32**:3095–3104.
26. Santangelo PJ, Nix B, Tsourkas A, Bao G. 2004. Dual FRET molecular beacons for mRNA detection in living cells. *Nucleic Acids Res* **32**(6):e57.
27. Alberts B, Johnson A, Lewis J, Raff M, Roberts K, Walter P. 2002. *Molecular biology of the cell*, 4th ed. Garland Science, New York.
28. Diaspro A, ed. 2002, *Confocal and two-photon microscopy, foundations, applications, and advances*. Wiley-Liss, New York.
29. Masters BR, Thompson BJ, eds. 2003. *Selected papers on multiphoton excitation microscopy*. SPIE Optical Engineering Press, Bellingham, Washington.
30. Zipfel WR, Williams RM, Webb WW. 2003. Nonlinear magic: multiphoton microscopy in the biosciences. *Nature Biotechnol* **21**(11):1369–1377.
31. Rigler R, Elson ES. 2001. *Fluorescence correlation spectroscopy*. Springer, Berlin.
32. Hegener O, Jordan R, Häberlein H. 2004. Dye-labeled benzodiazepines: development of small ligands for receptor binding studies using fluorescence correlation spectroscopy. *J Med Chem* **47**:3600–3605.
33. Rigler R, Orrit M, Basché T. 2001. *Single molecule spectroscopy*. Springer, Berlin.
34. Zander Ch, Enderlein J, Keller RA, eds. 2002. *Single molecule detection in solution, methods and applications*. Wiley-VCH, Darmstadt, Germany.
35. Li Q, Ruckstuhl T, Seeger S. 2004. Deep-UV laser-based fluorescence lifetime imaging microscopy of single molecules. *J Phys Chem B* **108**:8324–8329.
36. Ha T. 2004. Structural dynamics and processing of nucleic acids revealed by single-molecule spectroscopy. *Biochemistry* **43**(14):4055–4063.
37. Murakoshi H, Iino R, Kobayashi T, Fujiwara T, Ohshima C, Yoshimura A, Kusumi A. 2004. Single-molecule imaging analysis of Ras activation in living cells. *Proc Natl Acad Sci USA* **101**(19):7317–7322.
38. Kasha M. 1960. Paths of molecular excitation. *Radiation Res* **2**:243–275.
39. Hagag N, Birnbaum ER, Darnall DW. 1983. Resonance energy transfer between cysteine-34, tryptophan-214, and tyrosine-411 of human serum albumin. *Biochemistry* **22**:2420–2427.
40. O'Neil KT, Wolfe HR, Erickson-Viitanen S, DeGrado WF. 1987. Fluorescence properties of calmodulin-binding peptides reflect alpha-helical periodicity. *Science* **236**:1454–1456.
41. Johnson DA, Leathers VL, Martinez A-M, Walsh DA, Fletcher WH. 1993. Fluorescence resonance energy transfer within a heterochromatic cAMP-dependent protein kinase holoenzyme under equilibri-

um conditions: new insights into the conformational changes that result in cAMP-dependent activation. *Biochemistry* **32**:6402–6410.

A glossary of mathematical terms and commonly used acronyms is located at the end of this volume.

PROBLEMS

P1.1. *Estimation of Fluorescence and Phosphorescence Quantum Yields*: The quantum yield for fluorescence is determined by the radiative and non-radiative decay rates. The non-radiative rates are typically similar for fluorescence and phosphorescence states, but the emissive rates (Γ) vary greatly. Emission spectra, lifetimes (τ) and quantum yields (Q) for eosin and erythrosin B (ErB) are shown in Figure 1.13.

A. Calculate the natural lifetime (τ_n) and the radiative and non-radiative decay rates of eosin and ErB. What rate accounts for the lower quantum yield of ErB?

B. Phosphorescence lifetimes are typically near 1–10 ms. Assume that the natural lifetime for phosphorescence emission of these compounds is 10 ms, and that the non-radiative decay rates of the two compounds are the same for the triplet state as for the singlet state. Estimate the phosphorescence quantum yields of eosin and ErB at room temperature.

P1.2. *Estimation of Emission from the S_2 State*: When excited to the second singlet state (S_2) fluorophores typically relax to the first singlet state within 10^{-13} s.[38] Using the radiative decay rate calculated for eosin (problem 1.1), estimate the quantum yield of the S_2 state.

P1.3. *Thermal Population of Vibrational Levels*: The emission spectrum of perylene (Figure 1.3) shows equally spaced peaks that are due to various vibrational states, as illustrated. Use the Boltzmann distribution to estimate the fraction of the ground-state molecules that are in the first vibrationally excited state at room temperature.

P1.4. *Anisotropy of a Labeled Protein*: Naphthylamine sulfonic acids are widely used as extrinsic labels of proteins. A number of derivatives are available. One little known but particularly useful derivative is 2-diethylamino-5-naphthalenesulfonic acid (DENS), which displays a lifetime near 30 ns, longer than that of most similar molecules. Absorption and emission spectra of DENS are shown in Figure 1.36.

A. Suppose the fundamental anisotropy of DENS is 0.30 and that DENS is bound to a protein with a rotational correlation time of 30 ns. What is the anisotropy?

B. Assume now that the protein is bound to an antibody with a molecular weight of 160,000 and a rotational correlation time of 100 ns. What is the anisotropy of the DENS-labeled protein?

P1.5. *Effective Distance on the Efficiency of FRET*: Assume the presence of a single donor and acceptor and that the distance between them (r) can be varied.

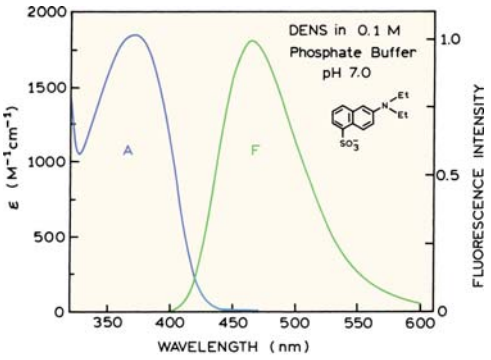

Figure 1.36. Absorption and emission spectra of DENS. The quantum yield relative to quinine sulfate is 0.84, and its lifetime is near 30 ns.

A. Plot the dependence of the energy transfer efficiency on the distance between the donor and the acceptor.

B. What is the transfer efficiency when the donor and the acceptor are separated by $0.5R_0$, R_0, and $2R_0$?

P1.6. *Calculation of a Distance from FRET Data*: The protein human serum albumin (HSA) has a single tryptophan residue at position 214. HSA was labeled with an anthraniloyl group placed covalently on cysteine-34.[39] Emission spectra of the labeled and unlabeled HSA are shown in Figure 1.37. The Förster distance for Trp to anthraniloyl transfer is 30.3 Å. Use the emission spectra in Figure 1.37 to calculate the Trp to anthraniloyl distance.

P1.7. *Interpretation of Tryptophan Fluorescence from a Peptide*: Figure 1.38 shows a summary of spectral data for a peptide from myosin light-chain kinase (MLCK). This peptide contained a single tryptophan residue, which was placed at positions 1 through 16 in the peptide. This peptide binds to the hydrophobic patch of calmodulin. Explain the changes in emission maxima, Stern-Volmer quenching constant for acrylamide (K), and anisotropy (r).

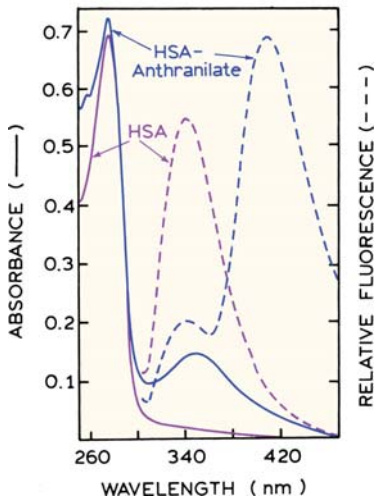

Figure 1.37. Absorption and fluorescence spectra of human serum albumin (HSA) and anthraniloyl-HSA. From [39].

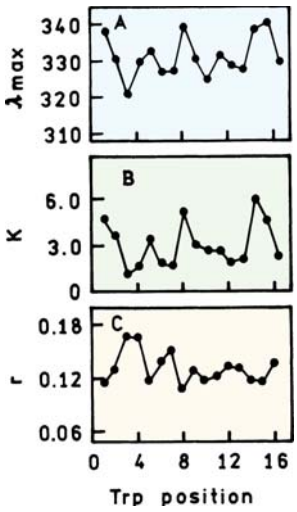

Figure 1.38. Dependence of the emission maxima (A), acrylamide quenching constants (B), and steady-state anisotropies (C) of MLCK peptides bound to calmodulin on the position of tryptophan residue. Reprinted, with permission, from [40]. (O'Neil KT, Wolfe HR, Erickson-Vitanen S, DeGrado WF. 1987. Fluorescence properties of calmodulin-binding peptides reflect alpha-helical periodicity. *Science* **236**:1454–1456, Copyright © 1987, American Association for the Advancement of Science.)

P1.8. *Interpretation of Resonance Energy Transfer Between Protein Subunits*: Figure 1.39 shows emission spectra of fluorescein (Fl) and rhodamine (Rh) when covalently attached to the catalytic (C) or regulator (R) subunit of a cAMP-dependent protein kinase (PK).[41] When the subunits are associated, RET occurs from Fl to Rh. The associated form is C_2R_2. Figure 1.40 shows emission spectra of both subunits without any additives, in the presence of cAMP, and in the presence of protein kinase inhibitor (PKI). Suggest an interpretation of these spectra. Your interpretation should be consistent with the data, but it may not be the only possible interpretation.

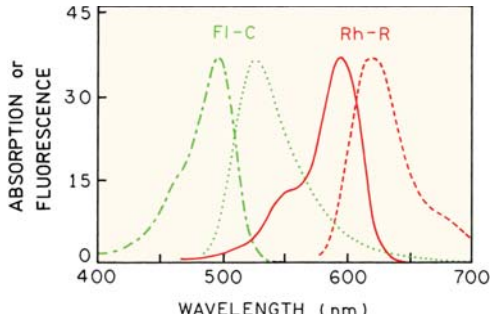

Figure 1.39. Spectral overlap of the fluorescein-labeled catalytic subunit (Fl-C) and the Texas red-labeled regulator subunit (Rh-R) of a cAMP-dependent protein kinase. Revised and reprinted with permission from [41]. (Copyright © 1993, American Chemical Society.)

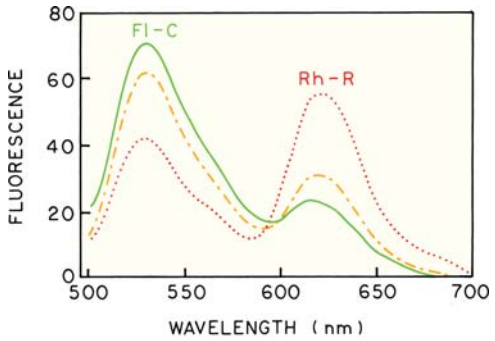

Figure 1.40. Effect of cAMP and the protein kinase inhibitor on the emission spectra of the donor and acceptor labeled holoenzyme. Emission spectra are shown without cAMP or PK (•••••), and the following addition of cAMP (–•–•), and PKI (——). Revised and reprinted with permission from [41]. (Copyright © 1993, American Chemical Society.)